

Reduction of outdoor particulate matter concentrations by local removal in semi-enclosed parking garages: a preliminary case study for Eindhoven city center

Citation for published version (APA):

Blocken, B., Vervoort, R., & van Hooft, T. (2016). Reduction of outdoor particulate matter concentrations by local removal in semi-enclosed parking garages: a preliminary case study for Eindhoven city center. *Journal of Wind Engineering and Industrial Aerodynamics*, 159, 80-98. <https://doi.org/10.1016/j.jweia.2016.10.008>

Document license:

CC BY-NC-ND

DOI:

[10.1016/j.jweia.2016.10.008](https://doi.org/10.1016/j.jweia.2016.10.008)

Document status and date:

Published: 26/10/2016

Document Version:

Publisher's PDF, also known as Version of Record (includes final page, issue and volume numbers)

Please check the document version of this publication:

- A submitted manuscript is the version of the article upon submission and before peer-review. There can be important differences between the submitted version and the official published version of record. People interested in the research are advised to contact the author for the final version of the publication, or visit the DOI to the publisher's website.
- The final author version and the galley proof are versions of the publication after peer review.
- The final published version features the final layout of the paper including the volume, issue and page numbers.

[Link to publication](#)

General rights

Copyright and moral rights for the publications made accessible in the public portal are retained by the authors and/or other copyright owners and it is a condition of accessing publications that users recognise and abide by the legal requirements associated with these rights.

- Users may download and print one copy of any publication from the public portal for the purpose of private study or research.
- You may not further distribute the material or use it for any profit-making activity or commercial gain.
- You may freely distribute the URL identifying the publication in the public portal.

If the publication is distributed under the terms of Article 25fa of the Dutch Copyright Act, indicated by the "Taverne" license above, please follow below link for the End User Agreement:

www.tue.nl/taverne

Take down policy

If you believe that this document breaches copyright please contact us at:

openaccess@tue.nl

providing details and we will investigate your claim.



Reduction of outdoor particulate matter concentrations by local removal in semi-enclosed parking garages: A preliminary case study for Eindhoven city center

Bert Blocken^{a,b,*}, Rob Vervoort^a, Twan van Hooff^{a,b}

^a Building Physics and Services, Department of the Built Environment, Eindhoven University of Technology, P.O. box 513, 5600 MB Eindhoven, The Netherlands

^b Building Physics Section, Department of Civil Engineering, KU Leuven, Kasteelpark Arenberg 40, bus 2447, 3001 Leuven, Belgium



ARTICLE INFO

Keywords:
Smart city
Air pollution
Air quality
Fine dust
Computational fluid dynamics (CFD)
Urban physics

ABSTRACT

Traffic is one of the main sources of particulate matter (PM) inside urban areas. This paper provides a preliminary assessment of the potential to reduce outdoor PM concentrations by local removal inside semi-enclosed parking garages. The assessment is performed by computational fluid dynamics (CFD) based on the 3D steady RANS equations and an Eulerian advection-diffusion equation. First, an extensive CFD validation study is performed with gas dispersion wind-tunnel measurements. Next, the case study for Eindhoven city center is conducted on a high-resolution grid including 16 semi-enclosed garages. Traffic intensities on the streets and in the garages are converted to PM₁₀ source terms. The garages are ventilated with outdoor air. Simulations are performed with and without removal units in the garages. The case study is not intended to reproduce a particular pollution episode but to provide a preliminary indication of the potential reduction in PM₁₀ for representative meteorological and traffic conditions. The results show that 594 removal units allow reductions in local outdoor PM₁₀ by up to 50% close to the garages while reductions up to 10% are achieved further downstream. It is concluded that local removal in semi-enclosed parking garages can be an effective strategy towards improved outdoor air quality.

1. Introduction

The World Health Organization states that particulate matter (PM) affects more people than any other pollutant and that it is strongly associated with human morbidity and mortality both daily and over time (WHO, 2014). While large particles when inhaled can be filtered in the nose and throat, particles smaller than about 10 micrometer (PM₁₀) can settle in the bronchi and lungs. Particles smaller than 2.5 micrometer (PM_{2.5}) can reach the alveoli, and particles less than 100 nanometer can pass through the lungs to other organs including the brain. Many studies have linked PM to lung cancer, respiratory, cardiovascular and cardiopulmonary diseases (e.g. Kunzli et al., 2000; Samet et al., 2000; Brunekreef and Holgate, 2002; Hoek et al., 2002; Pope and Dockery, 2006; Valavanidis et al., 2008; Raaschou-Nielsen et al., 2013; Beelen et al., 2014). Some have suggested links to stroke incidences and Alzheimer's and Parkinson's disease pathology (e.g. Block and Calderon-Garcidueñas, 2009; Ranft et al., 2009) while others have demonstrated the impact on birth outcomes (e.g. Brauer

et al., 2008; Pedersen et al., 2013). According to the Organization for Economic Cooperation and Development (OECD), by 2050 and without new policies, air pollution is set to become the world's top environmental cause of premature mortality. The number of premature deaths from exposure to PM is projected to more than double worldwide, from just over 1.5 million today to nearly 3.6 million per year in 2050 (OECD, 2012; EEA, 2015) (Fig. 1).

According to the Global Health Observatory, the mean concentration of PM₁₀ in urban areas ranges from less than 10 to over 200 µg/m³, and that of PM_{2.5} from less than 10 to over 100 µg/m³ (WHO, 2016). The WHO (2005) guideline has set limits aimed at achieving the lowest concentrations of PM possible: 20 µg/m³ annual mean and 50 µg/m³ 24-h mean for PM₁₀ and 10 µg/m³ annual mean and 25 µg/m³ 24-h mean for PM_{2.5}. Nevertheless, it acknowledges that the actual lower range of concentrations at which adverse health effects have been demonstrated is not greatly above the background concentration, which is estimated at 3–5 µg/m³ in the US and western Europe for PM_{2.5} (WHO, 2005). It is important to note that outdoor PM can be

* Corresponding author at: Building Physics and Services, Department of the Built Environment, Eindhoven University of Technology, P.O. box 513, 5600 MB Eindhoven, The Netherlands.

E-mail address: b.j.e.blocken@tue.nl (B. Blocken).

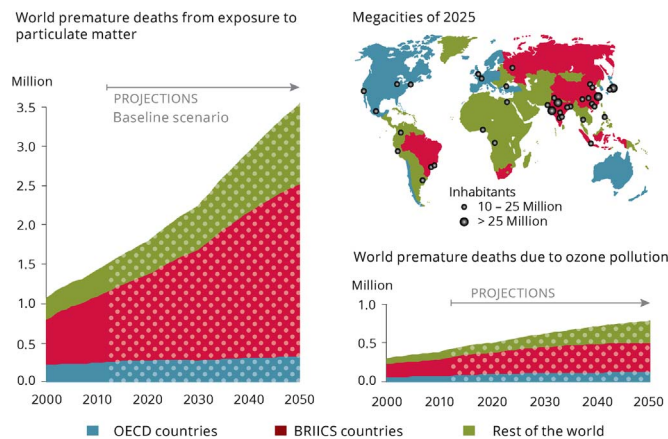


Fig. 1. Projected premature deaths due to particulate matter and ground-level ozone. BRIICS countries: Brazil, Russia, India, Indonesia, China, South Africa (EEA, 2015).

injected into buildings by mechanical and/or natural ventilation systems and by infiltration, dramatically increasing exposure times as most people spend 85–90% of their time indoors (Chen and Zhao, 2011).

The above-mentioned concentration values are averages over time acquired at specific locations. It should be noted that PM concentrations can show large gradients in space and time and that local instantaneous values can be substantially higher than the above-mentioned numbers. Especially traffic is an important source of PM and related morbidity and mortality (e.g. Brauer et al., 2008; Nordling et al., 2008; Pedersen et al., 2013) and it contributes both to background concentrations and to locally high concentrations of PM potentially far exceeding the above-mentioned limits. Traffic-related PM includes brake dust, tire wear and tailpipe emissions (e.g. Rogge et al., 1993). Local traffic-related PM concentrations are influenced by a wide range of parameters including urban and building geometry, traffic intensity and meteorological conditions. In particular in parking structures, PM concentrations have been found to be elevated relative to urban ambient levels (Kim et al., 2007; Zhang et al., 2008). Studies focused on PM in parking garages were mostly field studies (e.g. Majestic et al., 2009; Obaidullah et al., 2013; Samal et al., 2013; Vukovic et al., 2014). Majestic et al. analyzed the trace metal contents and iron isotope composition in a parking structure in Tempe, AZ, USA. They found extremely high levels of finer copper (up to 1000 ng/m³) likely from brake wear, and identified brake dust as the dominant source of iron in the parking garage. Obaidullah et al. (2013) measured PM concentrations and size distributions in three parking garages and two streets in Brussels, Belgium. They obtained average mass concentrations in the garages from 28 to 50 µg/m³ for PM₁, 43–60 µg/m³ for PM_{2.5} and 58–90 µg/m³ for PM₁₀, versus street values of 14–18 µg/m³ for PM₁, 23–27 µg/m³ for PM_{2.5} and 54–59 µg/m³ for PM₁₀, respectively. Samal et al. (2013) measured PM in an enclosed parking garage finding concentrations much higher than ambient values, with an average of 100 µg/m³ up to a maximum 234 µg/m³ for PM_{2.5}. Vukovic et al. (2014) reported measurements in four parking garages in Belgrade, Serbia. Concentrations exceeding 300 µg/m³ were measured. Apart from the latter study, garage and/or street geometry in these studies however were not described in detail.

The assessment of PM concentrations in urban areas can be attempted by on-site measurements, reduced-scale wind-tunnel measurements in an atmospheric boundary layer wind tunnel or by numerical simulation with computational fluid dynamics (CFD). Each of these approaches has particular advantages and disadvantages. The main advantage of on-site measurements is that they are able to capture the real complexity of the problem under study. Important disadvantages however are that they are not fully controllable due to – among others – the inherently variable meteorological conditions, that

they are not possible in the design stage of a building or urban area and that usually only point measurements are performed. The latter disadvantage also holds for wind-tunnel measurements. Techniques such as particle-image velocimetry (PIV) and laser-induced fluorescence (LIF) in principle allow planar or even full 3D data to be obtained in wind-tunnel tests, but the cost is considerably higher and application for complicated geometries can be hampered by laser-light shielding by the obstructions constituting the model, e.g. in case of an urban model consisting of many buildings. Another disadvantage is the required adherence to similarity criteria in reduced-scale testing, which can limit the extent and the range of problems that can be studied in wind tunnels. The use of CFD in wind engineering, also referred to as computational wind engineering (CWE), has seen a rapid growth in the past 50 years (see e.g. review and position papers by Murakami (1997), Stathopoulos (1997), Baker (2007), Solaro (2007), Meroney and Derickson (2014), Blocken (2014, 2015), Meroney (2016) and Tominaga and Stathopoulos (2016)). CWE/CFD has some particular advantages over experimental (full-scale or reduced-scale) testing. It can provide detailed information on the relevant flow variables in the whole calculation domain (“whole-flow field data”), under well-controlled conditions and without similarity constraints. However, the accuracy and reliability of CFD simulations are of concern and solution verification and validation studies are imperative.

In the past, CFD and wind-tunnel testing have been employed intensively for the study of – mainly gaseous – pollutant dispersion, see e.g. reviews by Robins (2003), Meroney (2004), Ahmad et al. (2005), Li et al. (2006), Blocken et al. (2011, 2013), Tominaga and Stathopoulos (2013, 2016), Di Sabatino et al. (2013) and Lateb et al. (2016). Many previous studies comparing CFD and wind-tunnel results have indicated that steady Reynolds-averaged Navier-Stokes (RANS) CFD simulations are deficient in accurately reproducing key features of the flow field around isolated bluff bodies such as separation, recirculation and von Karman vortex shedding in the wake (e.g. Paterson and Apelt, 1986, 1990; Murakami and Mochida, 1989; Murakami, 1990, 1993; Murakami et al., 1990, 1992; Rodi, 1997; Tominaga et al., 2008a; Shao et al., 2012; Tominaga, 2015; Liu and Niu, 2016). As a result, steady RANS simulations are generally also deficient in accurately reproducing pollutant dispersion around isolated buildings and one should resort to large eddy simulation (LES) even for obtaining reliable mean concentrations (e.g. Tominaga et al., 1997; Leitl et al., 1997; Li and Stathopoulos, 1997, 1998; Blocken et al., 2008a; Tominaga and Stathopoulos, 2009, 2010, 2013, 2016; Gousseau et al., 2011a, 2011b, 2012, 2015; Bazdidi-Tehrani et al., 2013; Ai and Mak, 2015). These validation studies indicated that deviations in mean concentrations between steady RANS simulations and wind-tunnel measurements can go up to a factor 10 or more. Similarly, it has been shown that steady RANS is generally deficient in accurately reproducing dispersion from roof top sources of buildings within urban areas (e.g. Gousseau et al., 2011b, 2015; Chavez et al., 2011, 2012) with similarly large deviations. However, quite some previous studies have also shown that steady RANS, in spite of its many limitations, can provide fairly accurate predictions of near-ground mean concentration fields by ground-level sources (generally less than factor 2 deviation) in densely built urban areas such as regular arrays of block-type buildings (e.g. Milliez and Carissimo, 2007; Dejoan et al., 2010; Tominaga and Stathopoulos, 2012; Efthimiou et al., 2015; Buccolieri et al., 2015). On the other hand, in less density built-up urban areas, much larger deviations are obtained (e.g. Flaherty et al., 2007).

As opposed to the very large amount of published CFD and wind-tunnel studies on dispersion of gases, much less studies have addressed the near-field dispersion of PM (e.g. Pospisil and Jicha, 2011; Fuka and Brechler, 2012; Tong et al., 2016a, 2016b). Several studies have focused on PM in parking garages, although – as mentioned earlier – most of these were field studies (e.g. Majestic et al., 2009; Obaidullah et al., 2013; Samal et al., 2013; Vukovic et al., 2014).

This paper presents a preliminary case study with CFD to assess the

potential of reducing the traffic-induced fraction of outdoor PM concentrations in urban areas by local removal by electrostatic precipitation/positive ionization inside semi-enclosed parking garages, where high PM concentrations can occur. First, a CFD validation study is conducted based on the wind-tunnel experiments by Garbero et al. (2010) of wind-induced gas dispersion in three types of buildings arrays, for different wind directions and for two values of the turbulent Schmidt number ($Sc_t=0.3$ and 0.7). Next, a CFD case study is performed for Eindhoven city center. The simulations are performed on a high-resolution and high-quality grid that includes the 16 below-ground and above-ground semi-enclosed parking garages. Three cases are considered: case 1 without removal units; case 2 with a total of 99 units; and case 3 with a total of 594 units inserted in the semi-enclosed parking garages. The paper is structured as follows. Section 2 describes the reasons for adopting the simplified PM dispersion modeling approach in this study. Section 3 presents the CFD validation study. Section 4 presents the case study for Eindhoven city center. Sections 5 and 6 present discussion and conclusions.

2. Simplified PM dispersion modeling

Given the complexity of the urban geometry, CFD is employed for flow and dispersion modeling. A distinction can be made between advanced modeling and simplified modeling. Advanced modeling takes into account chemical formation (nucleation) and aerosol dynamics (coagulation, condensation, etc), while simplified modeling excludes the specific treatment of aerosol dynamics and treats the particles as a gas. A review of dispersion modeling and its application to the dispersion of particles was provided by Holmes and Morawska (2006). The review states that the simplified models are capable of modeling the dispersion of particles in terms of $PM_{2.5}$ or PM_{10} since they are based on conservation of mass, but that they cannot readily provide information about particle number concentration. While differences between the advanced and the simplified approach can be substantial, especially very near to the source and for short averaging periods, Holmes and Morawska (2006) mention that since air quality regulations are currently based on particle mass concentrations, simplified models are essential. In addition, it is mentioned that “since several studies have shown a good correlation between non-reactive gases and particles within a larger airshed, validation studies involving gases should be a good indicator of the performance of the model in terms of calculations of particle mass concentrations.”

In the present paper, the simplified modeling approach is adopted. This is based on the above-mentioned statements, on previous CFD studies that have adopted the same approach and on the specific goal of this study. The goal is to compare the outdoor PM_{10} concentrations obtained in the cases with 99 and 594 removal units to those obtained in the case without units. The cases that are compared have the same traffic intensities and source terms, both inside and outside the semi-enclosed parking garages. The only difference is the number of units installed. A range of the systematic errors and uncertainties in the cases related to assumptions of traffic intensities and emissions are expected to act to a similar extent in all cases and to partially cancel out when concentration differences between the cases are considered. In addition, the traffic emission data being used already takes into account the near-source chemical formation and aerosol dynamics to some extent. The comparison is performed in a steady RANS framework which implies long averaging times. The local conditions that differ are especially the conditions in the parking garages, where PM exiting the garages is expected to have undergone substantial mixing inside before exiting. Note that a similar simplified approach to PM dispersion modeling was adopted by Fuka and Brechler (2012) for their validation study, by Guo and Maghirang (2012) for their case study, successfully validated with experiments and by Tong et al. (2016a, 2016b) and Jeanjean et al. (2016) for their case studies. Finally, Kumar et al. (2009) found a good agreement of modeling results with the

simplified approach with measured concentrations of nanoparticles in a street canyon.

3. CFD validation study

3.1. Wind-tunnel experiments

Based on the statement by Holmes and Morawska (2006) that validation studies involving gases should be a good indicator of the performance of the model in terms of calculations of particle mass concentrations, a validation study based on gas dispersion experiments is set up. Garbero et al. (2010) performed measurements of the dispersion of a passive tracer gas from a point source in idealized arrays of rectangular building models. Apart from the above-mentioned reason, these wind-tunnel experiments are selected for the CFD validation study because of three additional reasons: (1) their relevance and representativeness for the case study of Eindhoven city center (based on typical street widths and presence of mainly low-rise densely packed buildings downstream of the parking garages for southeast wind direction – see Section 4); (2) the availability of measurements for different street widths and different wind directions, hence going beyond the commonly studied case of wind direction parallel or perpendicular to the streets; and (3) the complete report of the experimental conditions which allows a detailed CFD validation study to be performed. The measurements were conducted in the closed-circuit atmospheric boundary layer wind tunnel of the Laboratoire de Mécanique des Fluides et d'Acoustique of the Ecole Centrale de Lyon in France. The wind tunnel has a test section of 14 m long, 3.7 m wide and 2.5 m high. A neutrally stratified turbulent boundary layer was generated by a combination of spires and roughness elements, where the roughness elements were identical in shape and size to the building models and covered the entire working section (Fig. 2) to avoid the development of an internal boundary layer. The resulting boundary layer had a height of about 0.8 m. The 1:400 reduced-scale building models had dimensions $L \times W \times H = 250 \times 250 \times 50 \text{ mm}^3$, corresponding to $L \times W \times H = 100 \times 100 \times 20 \text{ m}^3$ in full scale. The model roofs were each covered with 14 staggered “nuts” of 5 mm height representing roof-top structures. The reference wind speed at boundary-layer height was 5 m/s resulting in an obstacle Reynolds number (based on obstacle height and wind speed at that height) of 6700. Dispersion was studied for three different arrays: array A with street width in both directions S_x and S_y equal to H ; array B with $S_x=H$ and $S_y=2H$; and array C with $S_x=2H$ and $S_y=H$. For array A, results for different approach-flow wind directions were reported. The point source was placed in the middle of the intersection between two perpendicular streets at height $z/H=0.5$ and concentration measurements were made at $z/H=0.5$ and $z/H=2$. It was reported that the gas was quickly diluted and that passive diffusion started near the source (Garbero et al., 2010). Data were sampled for 120 s at a frequency of 300 Hz. The measurement uncertainty for the near-field mean concentrations was reported to be of the order of 3–5%



Fig. 2. Building array in the wind tunnel and indication of source position (Garbero et al., 2010).

while for the far-field mean concentrations it could reach 10% (Garbero et al., 2010).

3.2. CFD simulations: computational settings and parameters

The CFD simulations are performed with the 3D steady RANS equations supplemented with an Eulerian advection-diffusion equation. Closure for the RANS equations is obtained by the realizable k- ϵ model (Shih et al., 1995) and for the advection-diffusion equation with the standard gradient-diffusion hypothesis. The turbulent mass diffusivity results from $D_t = v_t/Sc_t$ with v_t the turbulent viscosity and Sc_t the turbulent Schmidt number. Two different values of Sc_t are used (0.3 and 0.7) in accordance with previous overview and review studies on gas dispersion (Tominaga and Stathopoulos, 2007, 2013). The simulations are performed at model scale. The computational geometry of the arrays resembles the geometry in the wind tunnel except for the upstream roughness elements (that have equal geometry as the building blocks) aligned with the wind-tunnel walls which are excluded (see Fig. 2). Array A consists of 12×15 buildings and arrays B and C of 10×14 buildings. The computational domains for arrays A, B and C have dimensions $L_D \times W_D \times H_D = 5.54 \times 4.55 \times 1.60 \text{ m}^3$, $5.15 \times 4.50 \times 1.60 \text{ m}^3$ and $5.80 \times 3.95 \times 1.60 \text{ m}^3$, respectively. The computational grids are developed according to best practice guidelines (Casey and Wintergerste, 2000; Tucker and Mosquera, 2001; Franke et al., 2004, 2007, 2011; Tominaga et al., 2008b; van Hooff and Blocken, 2010). A grid-convergence study indicates that for street width H , 10 cells across the street allow nearly grid-independent results (deviations in mean concentration below 5%) while for street width $2H$, 14 cells are required for similar grid convergence. The grids for arrays A, B and C are shown in Fig. 3 and contain 15×10^6 , 14×10^6 and 11×10^6 cells, respectively. The vertical inlet profiles of mean wind speed U and turbulent kinetic energy k are obtained from fitting

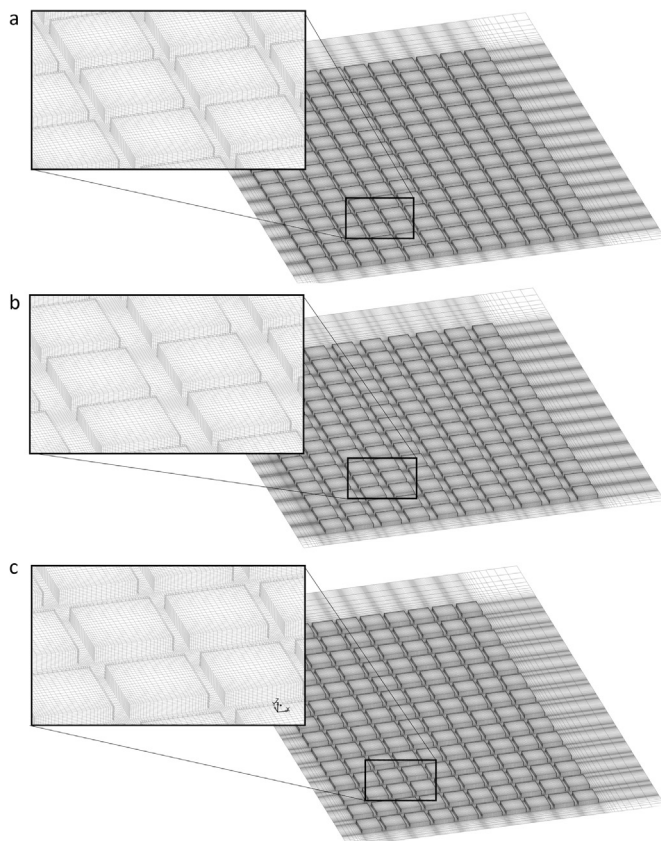


Fig. 3. Computational grids for (a) array A (15×10^6 cells); (b) array B (14×10^6 cells); and (c) array C (11×10^6 cells).

analytical functions to the values measured in the wind tunnel (Fig. 4). Fitting the log law to the mean wind speed measurements yields an aerodynamic roughness length $z_0 = 0.02 \text{ m}$ and a friction velocity $u^* = 0.552 \text{ m/s}$ for $U_{ref} = 5 \text{ m/s}$ at 0.8 m height. The turbulence dissipation rate ϵ is given by:

$$\epsilon(z) = \frac{u_{ABL}^{*3}}{\kappa(z + z_0)} \quad (1)$$

where κ is the von Karman constant (0.42). At the outlet, zero static pressure is specified. At the sides and the top of the domain, symmetry boundary conditions are imposed (i.e. zero normal velocity and gradients). At the surfaces of the streets, building walls and roofs, the standard wall functions by Launder and Spalding (1974) with the sand-grain roughness modification by Cebeci and Bradshaw (1977) are used. Simulations are performed for different values of surface roughness for the streets and the roofs. For the roofs, this includes taking into account the presence of the staggered nuts by Garbero et al. (2010) shown in Fig. 2 with an equivalent sand-grain roughness height of 0.001 m uniformly distributed over the entire roof surface. The same value is applied to the ground surface. However, the differences in mean concentration values in the street canyons at $z/H = 0.5$ (i.e. the focus of the validation study) with non-zero roughness compared to a simulation with zero surface roughness are consistently below 5%. Therefore only the results for zero surface roughness are presented in this paper. The passive pollutant source is modeled as a source term in the advection-diffusion equation with $0.01 \text{ kg/m}^3 \text{s}$ within a $0.01 \times 0.01 \times 0.002 \text{ m}^3$ volume in the middle of the street intersection where there are five building rows upstream, which is more than double the minimum of two rows required for pedestrian-level wind studies (Yoshie et al., 2007).

The CFD simulations are performed using the commercial CFD code ANSYS Fluent 14. The choice for the realizable k- ϵ turbulence model is based on the recommendations by Franke et al. (2004) and on earlier successful validation studies of pedestrian-level wind conditions by the authors (e.g. Blocken et al., 2004, 2007a, 2008b, 2012; Blocken and Persoon, 2009; Janssen et al., 2013; Topalar et al., 2015). Pressure velocity-coupling is taken care of by the SIMPLEC algorithm. Pressure interpolation is standard. Second-order discretization schemes are used for both the convection terms and viscous terms of the governing equations. Simulations are performed for the following wind directions: array A: $\theta = 2.5^\circ, 12.5^\circ, 27.5^\circ$; arrays B and C: $\theta = 2.5^\circ$. The iterations are terminated when the scaled residuals (ANSYS Inc., 2011) do not show any further reduction with increasing number of iterations. The following minimum values are reached: 10^{-7} for x-, y- and z-velocity, 10^{-5} for k and ϵ , 10^{-4} for continuity and 10^{-6} for concentration.

3.3. CFD simulations: results and validation

The results are presented as dimensionless concentration coefficients:

$$K = \frac{CU_H LH}{Q} \times 10^{-6} \quad (2)$$

where C is the mean concentration in ppm, Q is the pollutant emission rate in m^3/s , H and L are obstacle height and length and U_H the mean wind speed at height H . The results are shown as simulated versus measured profiles of K at height $z/H = 0.5$, which is the focus in this study as it is the line closest to pedestrian level. The results are given along horizontal lines at this height in the lateral streets and as simulated contours of K in a horizontal plane at the same height (Figs. 5–9). The following main observations are made:

- **Fig. 5:** For $\theta = 2.5^\circ$, the maximum concentrations are generally predicted with deviations less than a factor 2. The simulations with $Sc_t = 0.3$ (more turbulent diffusion) underestimate the street con-

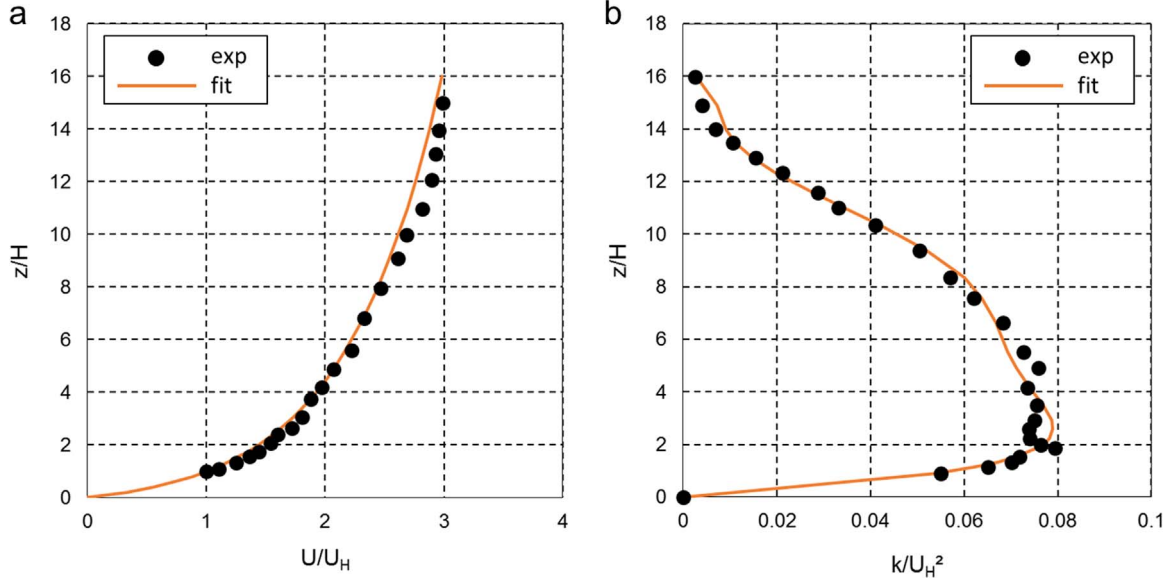


Fig. 4. Vertical profiles of dimensionless mean wind speed and turbulent kinetic energy as measured in the wind tunnel and fitted curves as input for CFD simulations.

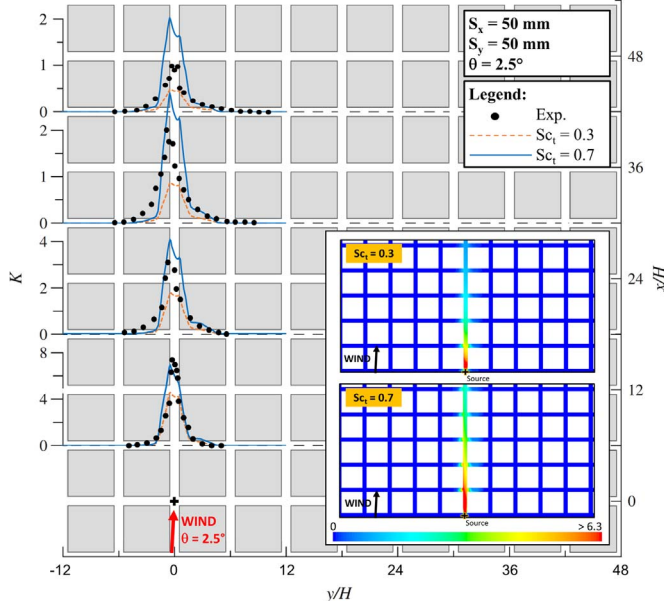


Fig. 5. Dimensionless concentration K by CFD simulations ($Sc_t=0.3$ and 0.7) and wind-tunnel measurements at height $z/H=0.5$ for equally spaced buildings and wind direction $\theta=2.5^\circ$. Source is indicated by +. Inserts are contours of K at height $z/H=0.5$.

centrations while those with $Sc_t=0.7$ (less turbulent diffusion) overestimate the street concentrations, except in the first street downstream of the source. Higher turbulent diffusion leads to more gas leaving the street canyons vertically and being evacuated by the flow over the building array. Plume spreading is underpredicted by both Sc_t values.

- **Fig. 6:** For $\theta=12.5^\circ$, similar observations are made about maximum concentrations as for $\theta=2.5^\circ$. However, spreading is better predicted for this more oblique wind direction, in particular the width of lateral spreading.
- **Fig. 7:** For $\theta=27.5^\circ$, the simulations with $Sc_t=0.3$ provide a good prediction of the magnitude of K (deviation less than factor 2) and the lateral spread for the 1st and 3rd street downstream of the source. However, for the 5th and 7th street, the magnitude is locally underestimated by a factor up to 3, while the length of the lateral dispersion/spread itself is accurately reproduced. The simulations with $Sc_t=0.7$ show a very different performance. While still accep-

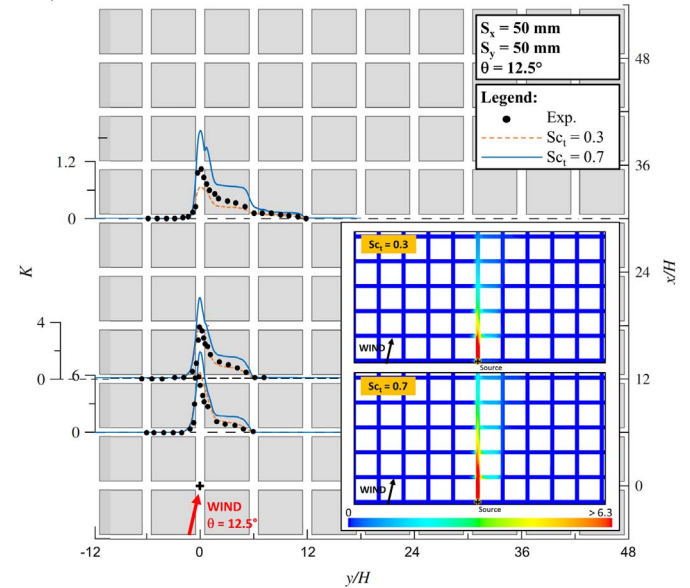


Fig. 6. Dimensionless concentration K by CFD simulations ($Sc_t=0.3$ and 0.7) and wind-tunnel measurements at height $z/H=0.5$ for equally spaced buildings and wind direction $\theta=12.5^\circ$. Source is indicated by +. Inserts are contours of K at height $z/H=0.5$.

table for the 1st and 3rd street, very large overestimations are provided for the 5th and 7th street, because this Sc_t value underestimates the vertical evacuation of the pollutant of out the street canyon and its subsequent removal by the flow over the array.

- **Fig. 8:** A wider street width in the along-wind direction yields a wider plume. Here, both the simulations with $Sc_t=0.3$ and 0.7 underestimate the maximum concentration. For $Sc_t=0.7$, the deviations are less than a factor 2, while for $Sc_t=0.3$, the deviations in the more downwind streets can go up to a factor 4. The extent of the lateral spread is accurately reproduced by both simulations.
- **Fig. 9:** A wider street width in the perpendicular direction yields a completely different dispersion pattern as in the previous cases. Downwind channeling is less pronounced while lateral channeling is stronger. The simulations with $Sc_t=0.3$ underestimate the maximum concentrations by a factor 2 up to 4, while those with $Sc_t=0.7$ reproduce the maxima within a factor 0.25. However, both simulations fail in accurately reproducing the extent of the lateral spread,

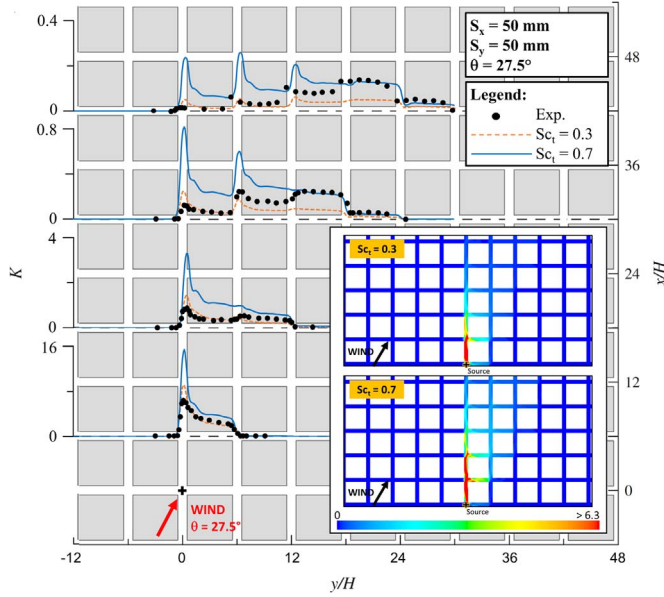


Fig. 7. Dimensionless concentration K by CFD simulations ($Sc_t=0.3$ and 0.7) and wind-tunnel measurements at height $z/H=0.5$ for equally spaced buildings and wind direction $\theta=27.5^\circ$. Source is indicated by +. Inserts are contours of K at height $z/H=0.5$.

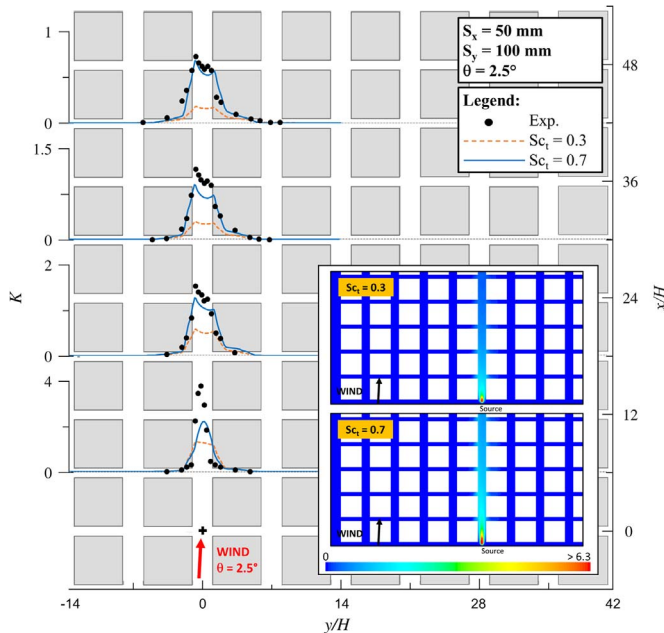


Fig. 8. Dimensionless concentration K by CFD simulations ($Sc_t=0.3$ and 0.7) and wind-tunnel measurements at height $z/H=0.5$ for unequally spaced buildings ($S_x=50$ mm, $S_y=100$ mm) and wind direction $\theta=2.5^\circ$. Source is indicated by +. Inserts are contours of K at height $z/H=0.5$.

although the predicted trend (skewness) in the 3rd and 5th street is good.

It can be concluded that there is no single Sc_t value that performs best for all cases investigated, which is in line with previous studies (e.g. Tominaga and Stathopoulos, 2007; Blocken et al., 2008a). This is not surprising as the appropriate value of the Sc_t number actually depends on the type of flow pattern and on the location in this flow pattern. However, apart from the case with $S_x=50$ mm, $S_y=100$ mm (Fig. 8), the measured concentrations are generally situated between the simulated concentrations by $Sc_t=0.3$ and $Sc_t=0.7$. Therefore, the current validation study will be used to support the CFD simulations for the case study of Eindhoven city center but these case study

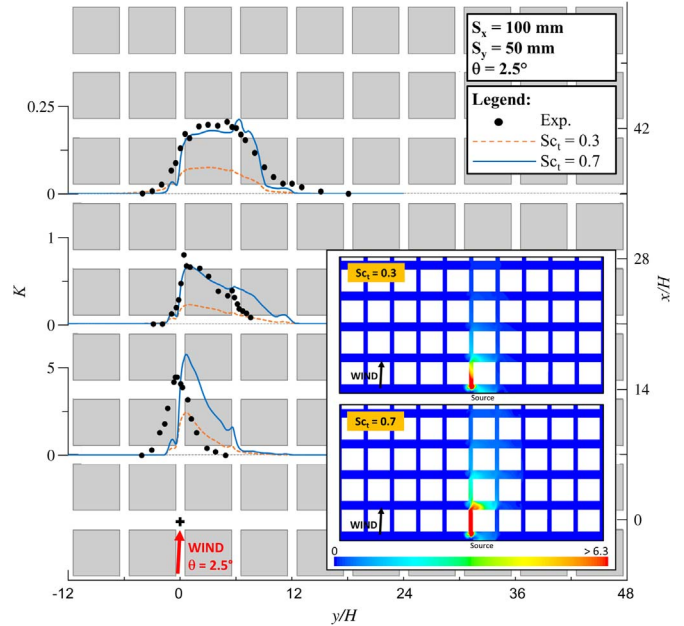


Fig. 9. Dimensionless concentration K by CFD simulations ($Sc_t=0.3$ and 0.7) and wind-tunnel measurements at height $z/H=0.5$ for unequally spaced buildings ($S_x=100$ mm, $S_y=50$ mm) and wind direction $\theta=2.5^\circ$. Source is indicated by +. Inserts are contours of K at height $z/H=0.5$.

simulations are performed for both $Sc_t=0.3$ and $Sc_t=0.7$, in order to provide an indication of the physical modeling uncertainty involved.

4. Case study

4.1. Study area and surroundings

Eindhoven is located in the south of the Netherlands in the province of North-Brabant. It is the 5th largest city of the Netherlands with about 225,000 inhabitants. The area of interest is the city center of Eindhoven, indicated by the dodecagon in Fig. 10 which covers an area of about 5.1 km². The city center is characterized by a mixture of commercial and residential buildings, which are mainly low-rise buildings with only a few high-rise buildings. Fig. 10b shows the 9 subareas and the location of the 16 semi-enclosed parking garages (labeled A to P), which are concentrated in the southwest part of the city center where the building density is highest. Fig. 11 illustrates the position of the dodecagon and the computational domain in the roughness map of the wider surroundings (circle with radius 10 km). The aerodynamic roughness length z_0 is estimated based on the Davenport-Wieringa roughness classification (Wieringa, 1992) and is shown in Fig. 11 for each of the 12 wind direction sectors. For the southeast wind direction under investigation, $z_0=0.5$ m.

4.2. Computational model, domain and grid

The buildings in the city center are modeled explicitly, although small facade and roof details are not included. Sidewalks, cars, benches and trees are not modeled explicitly but implicitly by increased values of the equivalent sand-grain roughness height for the streets and squares (see Section 4.3). The dimensions of the computational domain (Fig. 11) are $L \times W \times H = 4410 \times 3570 \times 600$ m³. Special care is given to the development of a high-quality and high-resolution grid that as much as possible satisfies the available best practice guidelines. The grid is constructed using the grid-generation technique presented by van Hooff and Blocken (2010), which allows a large degree of control over the quality of the grid and its individual cells. It consists of only hexahedral and prismatic cells and does not contain any tetrahedral or

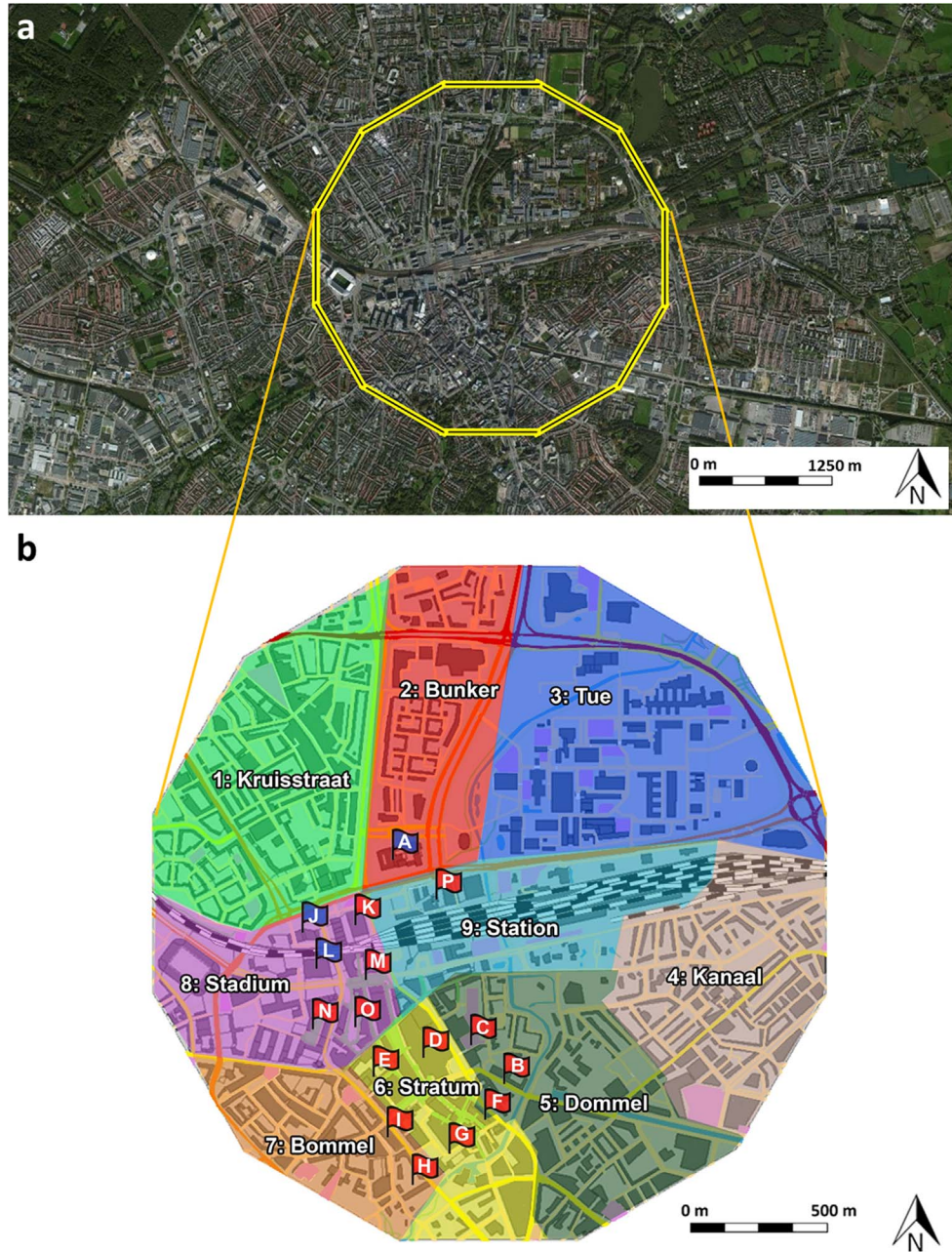


Fig. 10. (a) Area of interest (dodecagon) with explicitly modeled buildings. (b) Division of area of interest in 9 subareas and position of the 16 semi-enclosed parking garages A to P.

pyramid cells. Images of the grid are shown in Figs. 12–15. In particular, Fig. 15a–f illustrates some entrances of the parking garages, while Fig. 15g and h show details of entrances and ventilation outlets and Fig. 15i provides a view inside one of the semi-enclosed garages (G in Fig. 10) where an electrostatic precipitation/positive ionization removal unit is attached to the ceiling. While generating this type of grid that has only hexahedral and prism cells requires a considerable effort, it avoids the well-known convergence problems that are associated with steady RANS simulations on grids containing tetrahedral cells, especially when the required second-order discretization schemes are used. This advantage is considered very important, as first-order schemes should not be used due to their excessive contribution to numerical diffusion. This also corresponds to the guidelines by Franke et al. (2007), Tominaga et al. (2008b) and ASME (2011), who also recommend or even demand using higher-order discretization schemes. In accordance with the best practice guidelines (Franke et al., 2007; Tominaga et al., 2008b), five cell layers are provided below

pedestrian height (1.75 m), at which the results will be evaluated. The only exception to this are the below-ground parking garages. The resulting grid has about 65.7×10^6 hexahedral and prism cells.

4.3. Boundary conditions

The atmospheric boundary layer with neutral stratification is described by the vertical inlet profiles of mean wind speed U , turbulent kinetic energy k and turbulence dissipation rate ε by Richards and Hoxey (1993):

$$U(z) = \frac{u_{ABL}^*}{\kappa} \ln \left(\frac{z + z_0}{z_0} \right) \quad (3)$$

$$k(z) = \frac{u_{ABL}^{*2}}{\sqrt{C_\mu}} \quad (4)$$

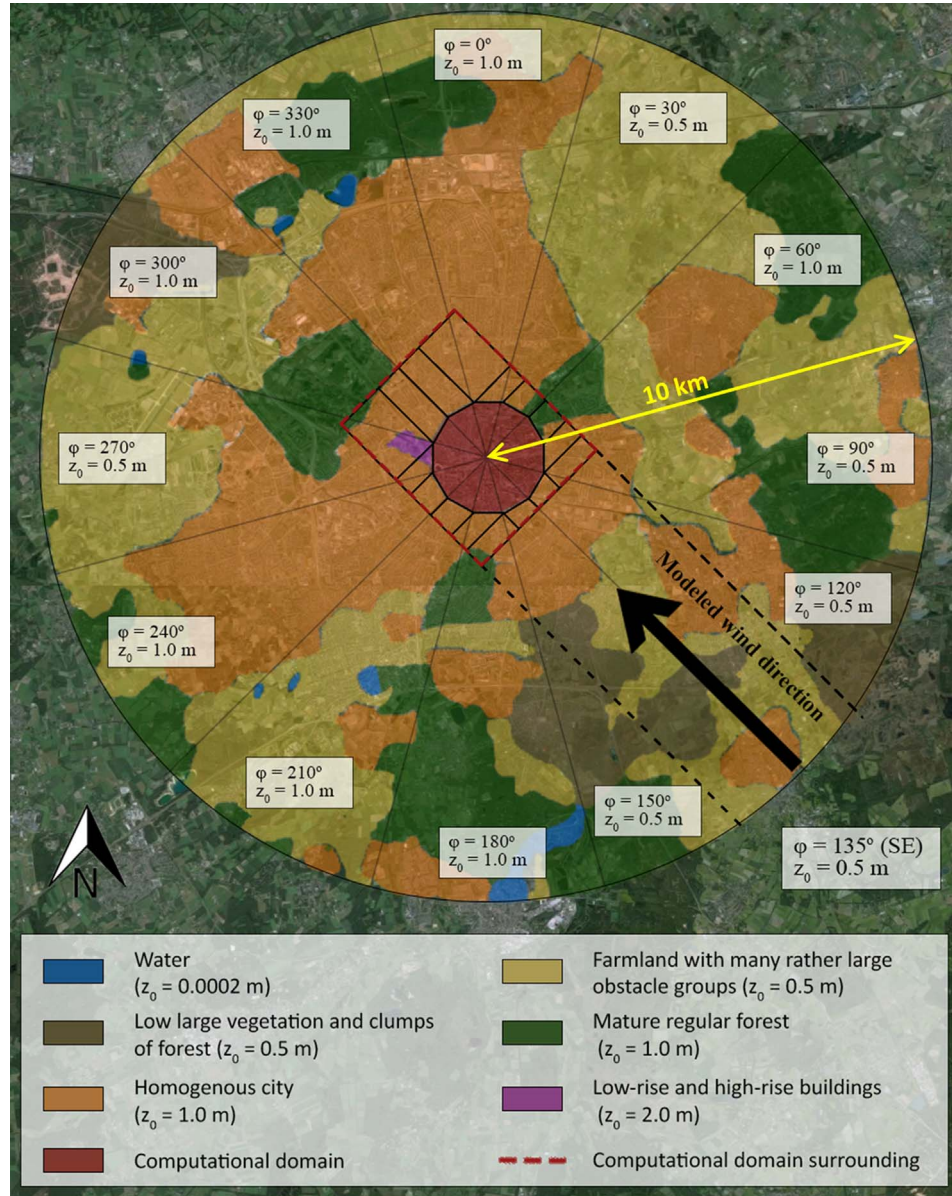


Fig. 11. Position of area of interest and computational domain in 10 km radius circle with aerodynamic roughness classification of surrounding area.

$$\varepsilon(z) = \frac{u_{ABL}^*}{\kappa} \frac{z^3}{(z + z_0)} \quad (5)$$

where z_0 is the aerodynamic roughness length of the terrain upstream of the computational domain ($z_0=0.5 \text{ m}$ for SE wind direction – see Fig. 11) and C_μ a constant equal to 0.09. The reference wind speed is 1 m/s at 10 m height. The inlet concentration of PM_{10} is obtained from the measurement station of Veldhoven situated southeast of the area of interest, at a distance of approximately 6 km from the city center. The hourly average value of $\text{PM}_{10}=17.3 \mu\text{g}/\text{m}^3$ is imposed. At the outlet of the domain, zero static pressure is specified. At the sides and the top of the domain, symmetry boundary conditions are imposed (i.e. zero normal velocity and gradients). At the surfaces of the streets, building facades and building roofs, the standard wall functions by Launder and Spalding (1974) with the sand-grain roughness modification by Cebeci and Bradshaw (1977) are used. For the building walls and roofs, an equivalent sand-grain roughness height $k_s=0.1 \text{ m}$ and roughness constant $C_s=0.5$ are imposed. For the streets, an aerodynamic roughness length of $z_0=0.03 \text{ m}$ is imposed, taking into account benches, sidewalks, trees, etc. This value originates from an earlier CFD

validation study (Blocken and Persoon, 2009). For the bottom of the computational domain outside the dodecagon, where the buildings are not modeled explicitly, $z_0=0.5 \text{ m}$ is imposed, in order to avoid unintended streamwise gradients in the approach-flow profiles. As the wall functions require values of k_s and C_s rather than z_0 , the following conversion equation that was derived by Blocken et al. (2007b) for ANSYS Fluent, is used:

$$k_{S,ABL} = \frac{9.793}{C_s} \frac{z_0}{C_s} \quad (6)$$

The resulting values of k_s and C_s are 0.042 m and 7 for the streets, and 0.7 m and 7 for the bottom of the domain outside the dodecagon.

Traffic exhaust is implemented by pollutant source terms in the streets and in the parking garages. Traffic intensity data for the streets is obtained from the municipality of Eindhoven (Eindhoven Municipality, 2015). The daily number of motorized vehicles for the main streets on an average week day is shown in Fig. 16. This number is converted to the number of driven kilometers, after which the PM emission table from Rijkswaterstaat, i.e. the Ministry of Infrastructure and the Environment, for city traffic-related burnt fuel and mechanical

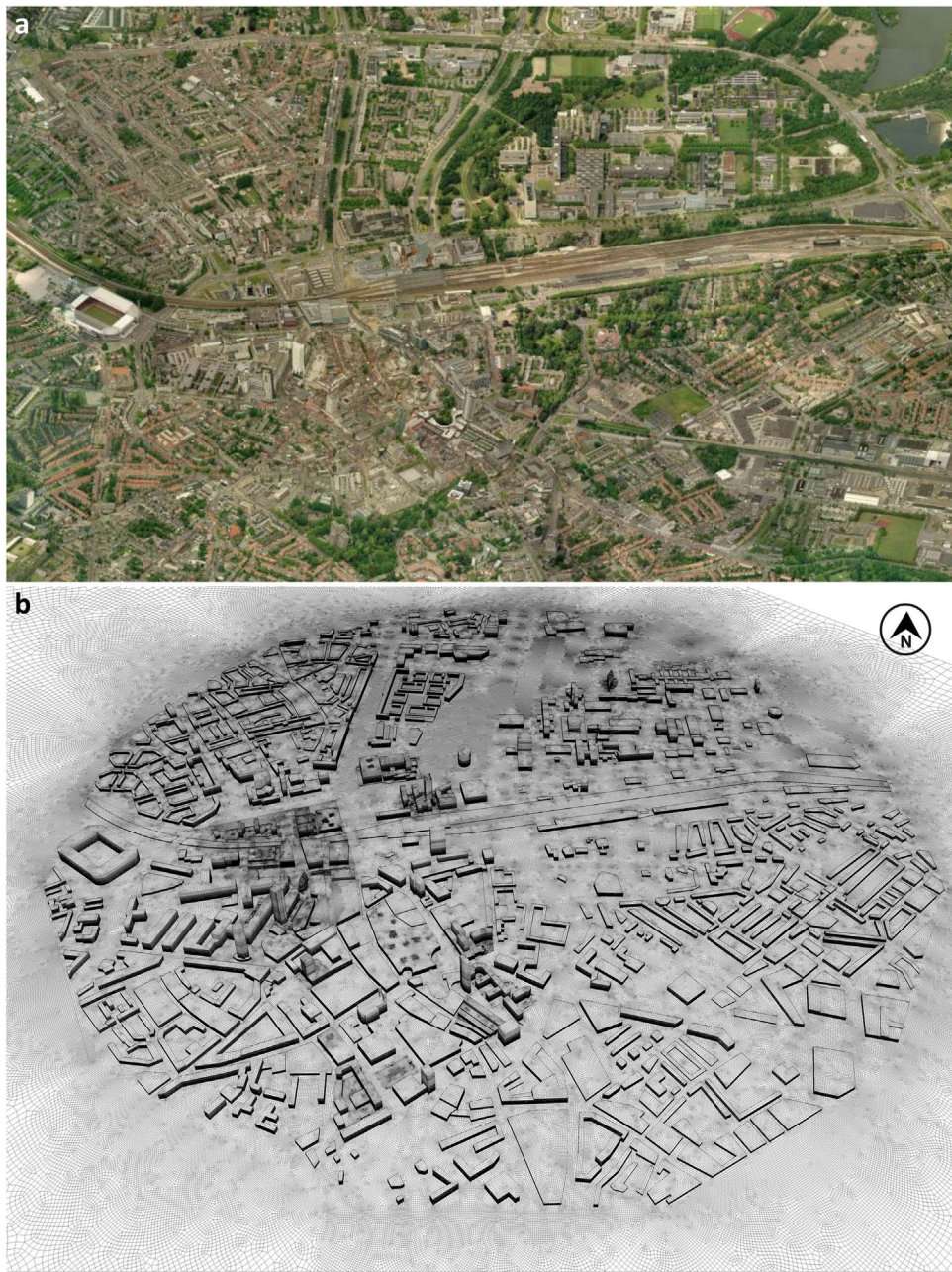


Fig. 12. (a) Aerial photograph of Eindhoven city center from south. (b) Corresponding view of computational grid on and around explicitly modeled buildings (65.7×10^6 cells).

wear (Table 1) is employed to yield the corresponding estimates of PM₁₀ and PM_{2.5} (Rijkswaterstaat, 2016). In Table 1, stagnant city traffic refers to traffic with a high degree of congestion, an average speed of less than 15 km/h and on average about 10 stops per km. Normal city traffic is traffic with a reasonable degree of congestion, an average speed between 15 and 30 km/h and on average about 2 stops per km. Smooth city traffic is traffic with a relatively large fraction of “free-flow” behavior, with an average speed between 30 and 45 km/h and on average about 1.5 stops per km. For the calculation of the emissions in the streets of Eindhoven, the case of normal city traffic is used. As the traffic intensity data in Fig. 16 relates to a 24-h period, more realistic source terms are obtained by assuming the PM to be emitted in a time frame of 10 h. The added sources for all streets in every subarea in Fig. 16 are equally distributed over all streets in this subarea. Note that this approach is more detailed than in recent studies (e.g. Jeanjean et al., 2016) where uniform distribution over all streets is assumed. For every street, the source terms are imposed in a volume

with width equal to the street width and height from 0 to 1.5 m. The equal spreading attempts to take into account the local dispersion due to traffic-induced turbulence. The values of the source terms for each of the 9 subareas are presented in Table 2. For the subarea ‘Tue’, which is the university campus, the source term was put to 0. In the largest part of this subarea, the traffic intensity is very low. However the ring road around Eindhoven city center crosses this subarea near its border, which would result in an unrealistically high amount of driven km equally distributed over this subarea. Given the southeast wind direction, the emitted PM₁₀ from this part of the ring road will be transported out of the area of interest anyway, therefore the above assumption is considered appropriate.

For the parking garages, estimates of PM₁₀ emissions are made based on the combination of the following parameters: (1) number of parking spots, (2) number of vehicles using the parking over a 24-h duration, (3) estimate of average duration for a car to drive into the parking garage, find a spot, and afterwards leave the garage (depending

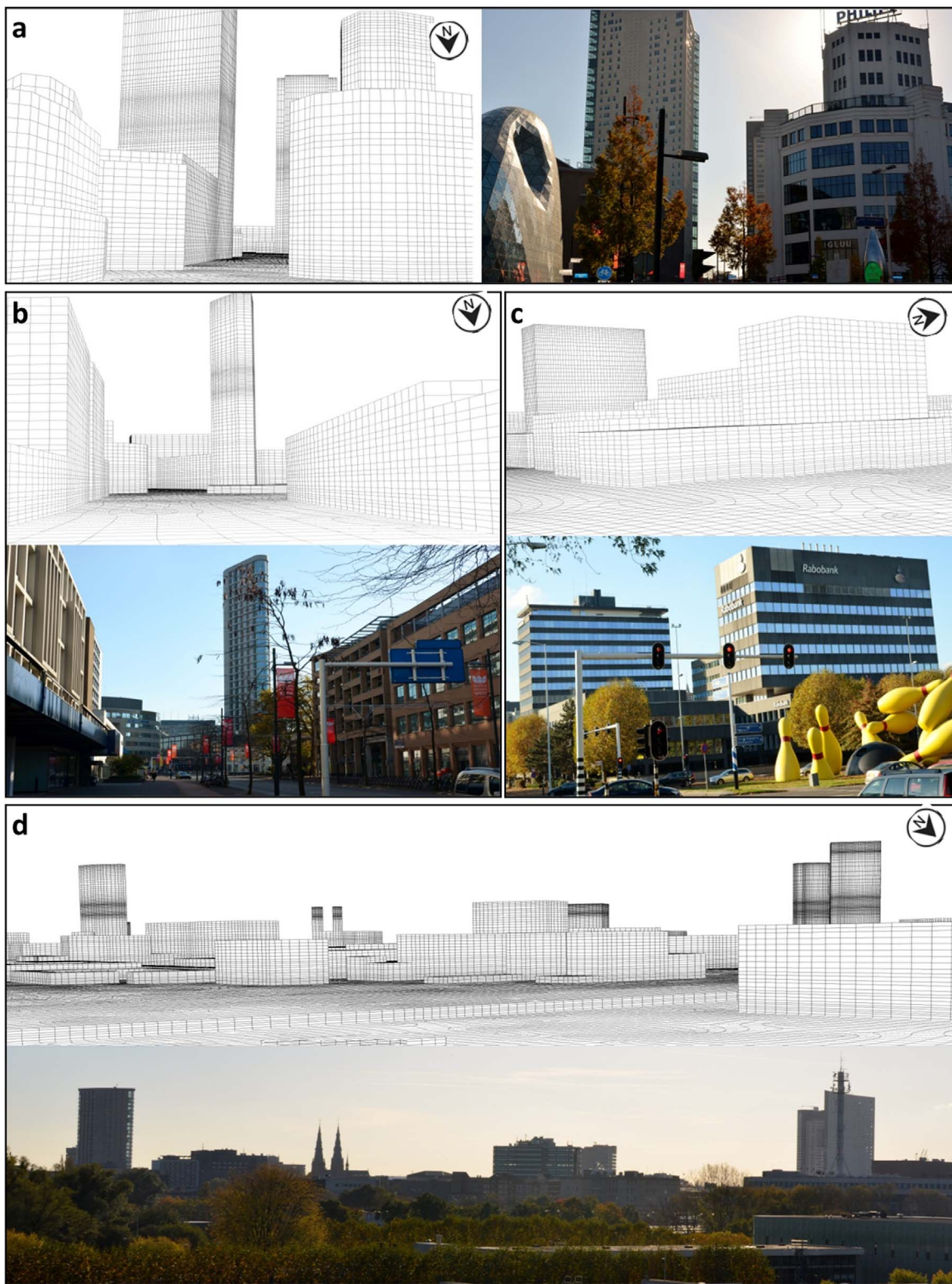


Fig. 13. Photographs of some parts of Eindhoven city center and corresponding views of computational grid on and around explicitly modeled buildings.

on size of the garage this estimate was set to 6 up to 14 min), (4) estimate of average vehicle speed in parking garage (set at 8 km/h). Based on this information and these estimates, the number of driven km inside the garages is obtained where again the average is taken over 10 h instead of 24. These numbers are combined with the emission table (Table 1) for stagnant traffic, only considering passenger cars, yielding the results in Table 3. Note that garage M is omitted as it is only used for bicycles. The emissions are uniformly distributed over the

entire garage volume, assuming efficient mixing of PM₁₀ due to vehicle-induced turbulence and internal airflow by the garage ventilation system. The parking garages themselves are included in detail in the computational model, both concerning geometry including removal units (see Figs. 15 and 17) and boundary conditions (see Fig. 17). The ventilation of the parking garages is imposed according to the Dutch national building guideline (NEN, 2001) that demands a ventilation rate of 10.8 m³/m² h. The total ventilation rate is distributed over the



Fig. 14. Photographs of some parts of Eindhoven city center and corresponding views of computational grid on and around explicitly modeled buildings.

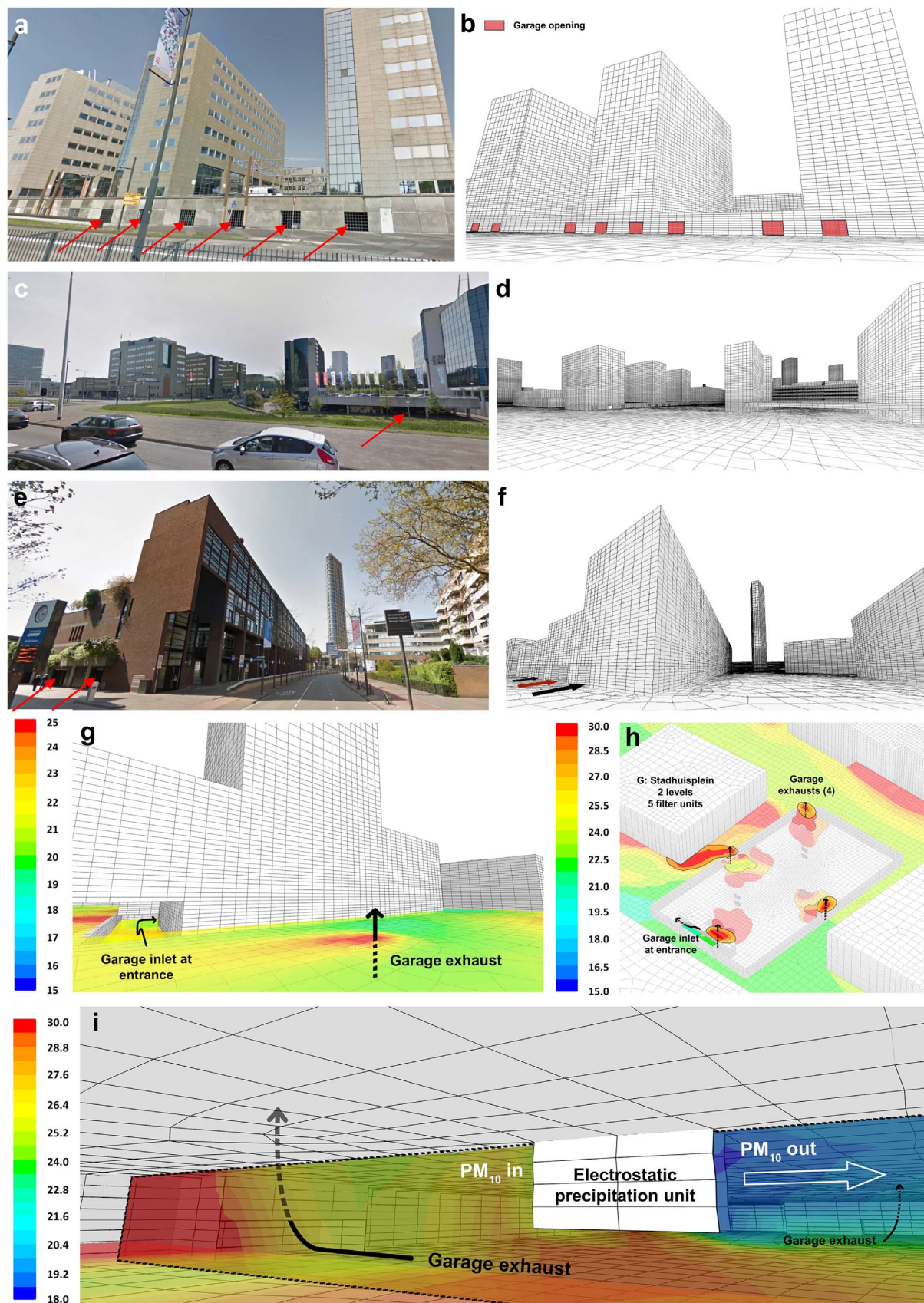


Fig. 15. (a-f) Photographs of some semi-enclosed parking garages in Eindhoven city center and corresponding views of computational grid. Garage entrances and/or ventilation openings are indicated with arrows. (g-h) Details of computational grid near and in parking garages. Contours are PM₁₀ concentration in $\mu\text{g}/\text{m}^3$. (i) Detail of computational grid and electrostatic precipitation unit inside underground parking garage. Contours are PM₁₀ concentration in $\mu\text{g}/\text{m}^3$.

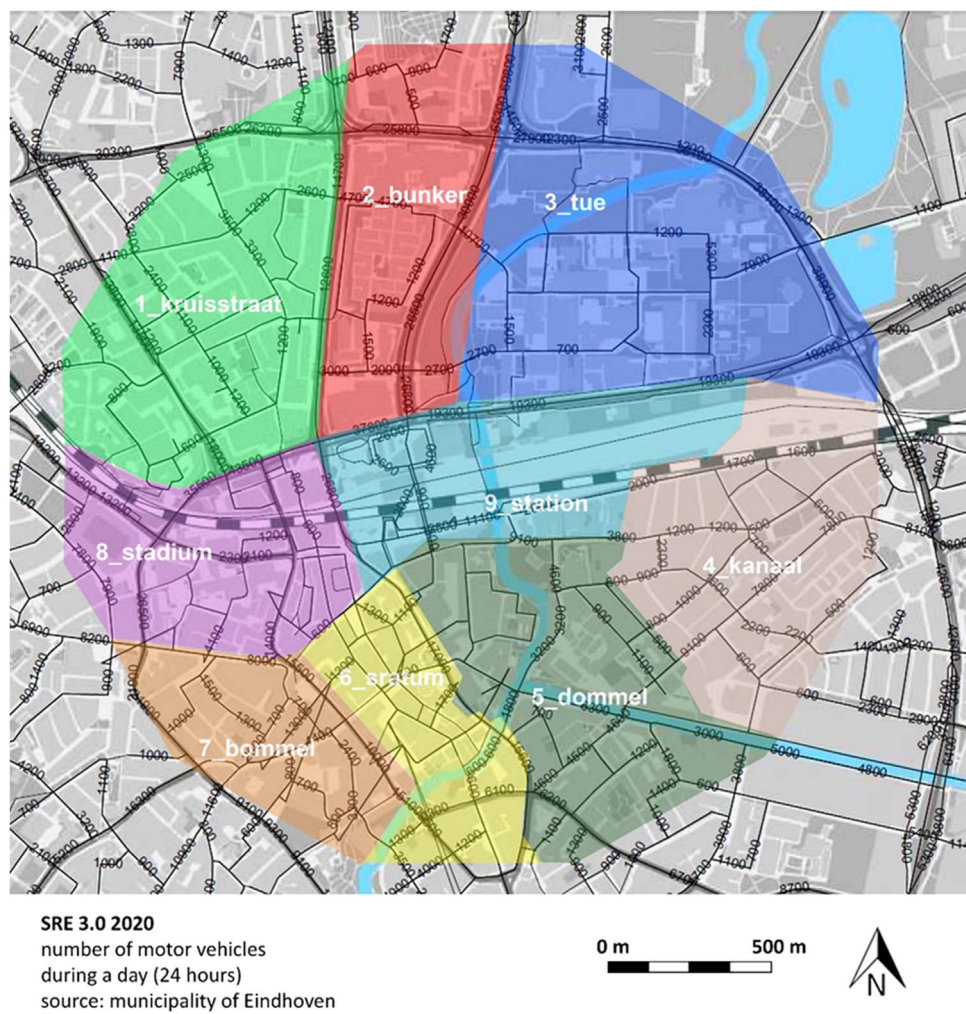


Fig. 16. Predicted number of motorized vehicles on main roads during an average weekly day.

Table 1
Total emission of PM₁₀ and PM_{2.5} from burning fuel and mechanical wear (Rijkswaterstaat, 2016).

	Traffic in urban areas		City stagnant (g/km)		City normal (g/km)		City smooth (g/km)	
	10 ⁶ km	%	PM ₁₀	PM _{2.5}	PM ₁₀	PM _{2.5}	PM ₁₀	PM _{2.5}
Road traffic – total	26561	100.0%	0.0461	0.0228	0.0423	0.0183	0.0414	0.0174
Passenger cars	20954	78.9%	0.0390	0.0184	0.0370	0.0158	0.0370	0.0158
Motorcycles	387	1.5%	0.0390	0.0184	0.0370	0.0158	0.0370	0.0158
Mopeds	1570	5.9%	0.0390	0.0184	0.0370	0.0158	0.0370	0.0158
Vans	2643	10.0%	0.0390	0.0184	0.0370	0.0158	0.0370	0.0158
Lorries	413	1.6%	0.2254	0.1234	0.1810	0.0790	0.1586	0.0566
Tractors	269	1.0%	0.2462	0.1512	0.1898	0.0948	0.1632	0.0682
Buses	248	0.9%	0.2048	0.1278	0.1498	0.0728	0.1250	0.0480
Special vehicles – total								
Light	22	0.1%	0.2254	0.1234	0.1810	0.0790	0.1586	0.0566
Heavy	55	0.2%	0.2462	0.1512	0.1898	0.0948	0.1632	0.0682

ventilation openings and imposed by assigning fixed values for the velocity as shown in Fig. 16. Finally, for case 2 (99 units) and case 3 (594 units), the electrostatic precipitation/positive ionization removal units are virtually implemented in the parking garages (see Figs. 15 and 17). The units are commercially available and called Aufero (ENS, 2016a). They have dimensions L×W×H = 2.50×0.69×1.37 m³ with a maximum volume flow rate of 9000 m³/h. The particle removal efficiency for a clean unit is assumed to be 70% for PM₁₀ (ENS, 2016b). For every unit, the 9000 m³/h and removal efficiency of 0.7 are imposed with a user-defined function (ANSYS Inc., 2011). For case 2,

one unit is applied per 65 parking spots, yielding a total of 99 units distributed over 15 parking garages. For case 3, six units are applied per 65 spots, yielding a total of 594 units.

4.4. Solver settings

The 3D steady RANS equations and the advection-diffusion equation are solved with the commercial CFD code Fluent 14. The simulations are isothermal. Pressure velocity-coupling is taken care of by the SIMPLEC algorithm. Pressure interpolation is standard.

Table 2Data for estimation of PM₁₀ emission in streets for every subarea in Fig. 10.

Nr.	Name	Volume (m ³)	d (km)	PM ₁₀ (10 ⁻² µg/m ³ s)
1	Kruisstraat	796154	44381	6.55
2	Bunker	666071	67650	11.93
3	Tue	644521	90706	0
4	Kanaal	644250	11865	2.16
5	Dommel	653054	23845	4.29
6	Stratum	263611	18433	8.22
7	Bommel	314843	21761	8.12
8	Stadium	441384	52830	14.06
9	Station	439928	33616	8.98

Second-order discretization schemes are used for both the convection terms and viscous terms of the governing equations. The simulations are performed on a 16 core machine with 2.90 GHz processors and 256 GB memory. Every simulation takes about 18,000 iterations and lasts for about 10 days. The iterations are terminated when the scaled residuals (ANSYS Inc., 2011) do not show any further reduction with increasing number of iterations. The following minimum values are reached: 10⁻⁶ for x-, y- and z-velocity, 10⁻⁵ for k and ε, 10⁻⁴ for continuity and 10⁻⁵ for concentration.

4.5. Simulation results

Fig. 18 presents contours of outdoor PM₁₀ concentration in a horizontal plane at z=1.75 m, i.e. pedestrian level, for case 1 without removal units (reference case; Fig. 18a–d) and case 3 with 594 removal units (18e–h) as obtained with the simulations with Sc_t=0.7. Note that the upper limit of the colorbar has been set at 40 µg/m³ for visualization purposes but that the actual concentrations occurring are higher and exceed 50 µg/m³. Nevertheless, the maximum concentrations are relatively limited as a result of the boundary conditions: the combination of averaging emissions in space (over subareas) and in time (equal distribution over 10 h) and a reference wind speed of 1 m/s. It is expected that during rush hours and/or for lower wind speed conditions, local concentrations will be higher. Comparing the results of case 1 and case 3, it is clear that the parking garages accumulate PM₁₀ that is then exhausted into the outdoor environment through the relatively small ventilation openings, yielding high concentrations especially in the vicinity of these openings. The addition of the removal units evidently reduces the indoor PM₁₀ concentration and the PM₁₀ concentration in the exhaust flow. While this effect is limited for some of the garages (Fig. 18b vs. f), its is – at least near the ventilation outlets – substantial for others (Fig. 18c vs. g and Fig. 18d vs. h).

Table 3Data for estimation of PM₁₀ emissions in parking garages. Garage M is omitted as it is only used for bicycles.

Code	Name	Subarea	Volume (m ³)	Parking spots	Vehicles	t _{in-out} (min)	d (km)	PM ₁₀ (10 ⁻² µg/m ³ s)
A	Rabobank	2	31505	250	750	8	800	2.75
B	Lagelanden/Marienhage	5	26637	355	1065	8	1136	4.62
C	Pullman Hotel	5	8265	50	100	5	67	0.88
D	Heuvelgalerie	6	143989	1106	4424	12	7078	5.33
E	Hooghuys	6	22924	195	585	7	546	2.58
F	Medina complex	6	19128	264	792	7	739	4.19
G	Stadhuisplein	6	20530	314	942	8	1004	5.30
H	Stadskantoor	7	20973	265	795	8	848	4.38
I	De Nieuwe Wal	7	14501	180	540	8	576	4.30
J	Parkeerdek 't Eindje	8	31801	350	1050	6	840	2.86
K	Bijenkorf	8	42078	584	2336	10	3114	8.02
L	Mathildelaan	8	111443	1187	4748	14	8862	8.61
N	Witte Dame/Lichttoren	8	35834	509	1527	8	1628	4.92
O	Admirant	8	25070	314	942	8	1004	4.34
P	Kennedyplein	8	72606	799	2397	10	3196	4.77

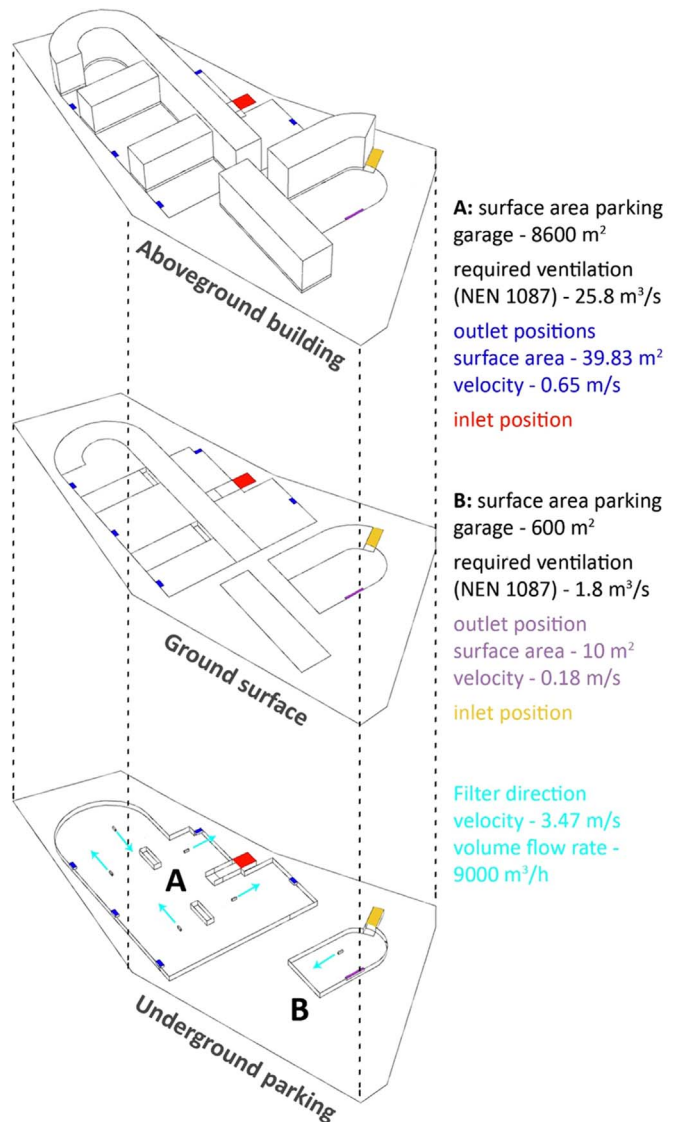


Fig. 17. Computational geometry of a parking garage (B: Lagelanden+Marienhage) with PM removal units and indication of ventilation inlet and outlet openings.

Fig. 19 presents the reduction of outdoor PM₁₀ concentration in a horizontal plane at 1.75 m height for case 2 and case 3, relative to case 1, for Sc_t=0.3. It indicates that for case 2 (99 units), very locally around

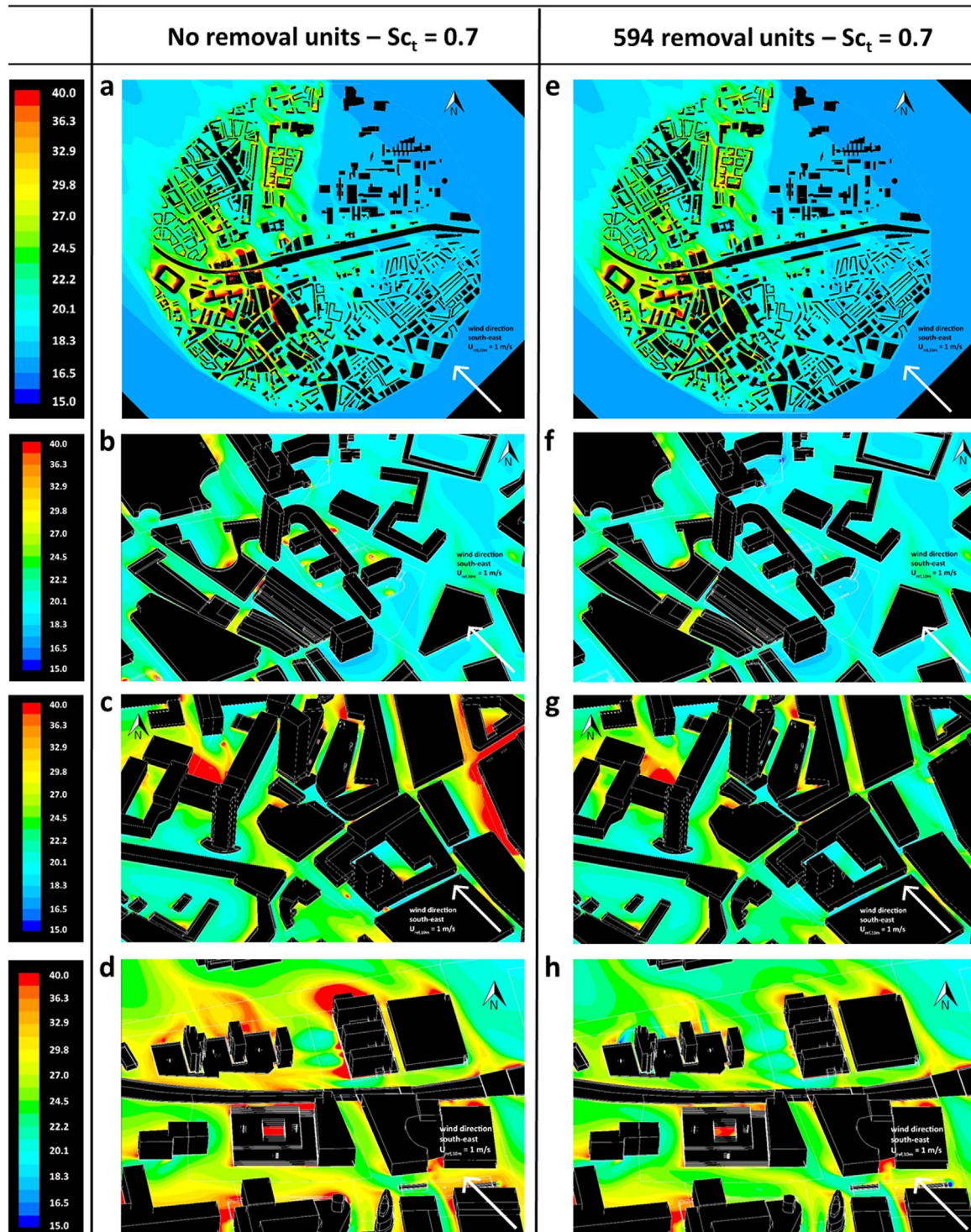


Fig. 18. Contours of outdoor PM₁₀ concentration ($\mu\text{g}/\text{m}^3$) in horizontal plane at 1.75 m height for $\text{Sc}_t=0.7$. (a-d) Without removal units. (e-h) With 594 removal units installed in the semi-enclosed parking garages.

the parking garages, reductions up to at least 10% can be seen. However, reductions farther away are very small to indiscernible. For case 3 (594 units) however, a much larger area around some of the parking garages shows reductions up to at least 10% (Fig. 19c), with very locally peak reductions reaching 50% (Fig. 19d). Fig. 19c illustrates that the plume of air with lower PM₁₀ concentration is convected downstream along the wind direction. Fig. 20 presents similar graphs but for $\text{Sc}_t=0.7$. As also shown in the validation study in Section 3, the streamwise concentration gradients for $\text{Sc}_t=0.7$ are less pronounced than for $\text{Sc}_t=0.3$, which is mainly attributed to the stronger vertical

dispersion for $\text{Sc}_t=0.3$.

5. Discussion

This paper has presented a preliminary assessment of the potential to reduce the traffic-induced fraction of outdoor PM concentration in urban areas by local removal by electrostatic precipitation/positive ionization inside semi-enclosed parking garages. The assessment is considered preliminary because of several assumptions made, in particular concerning the steady framework, the equal spatial spread-

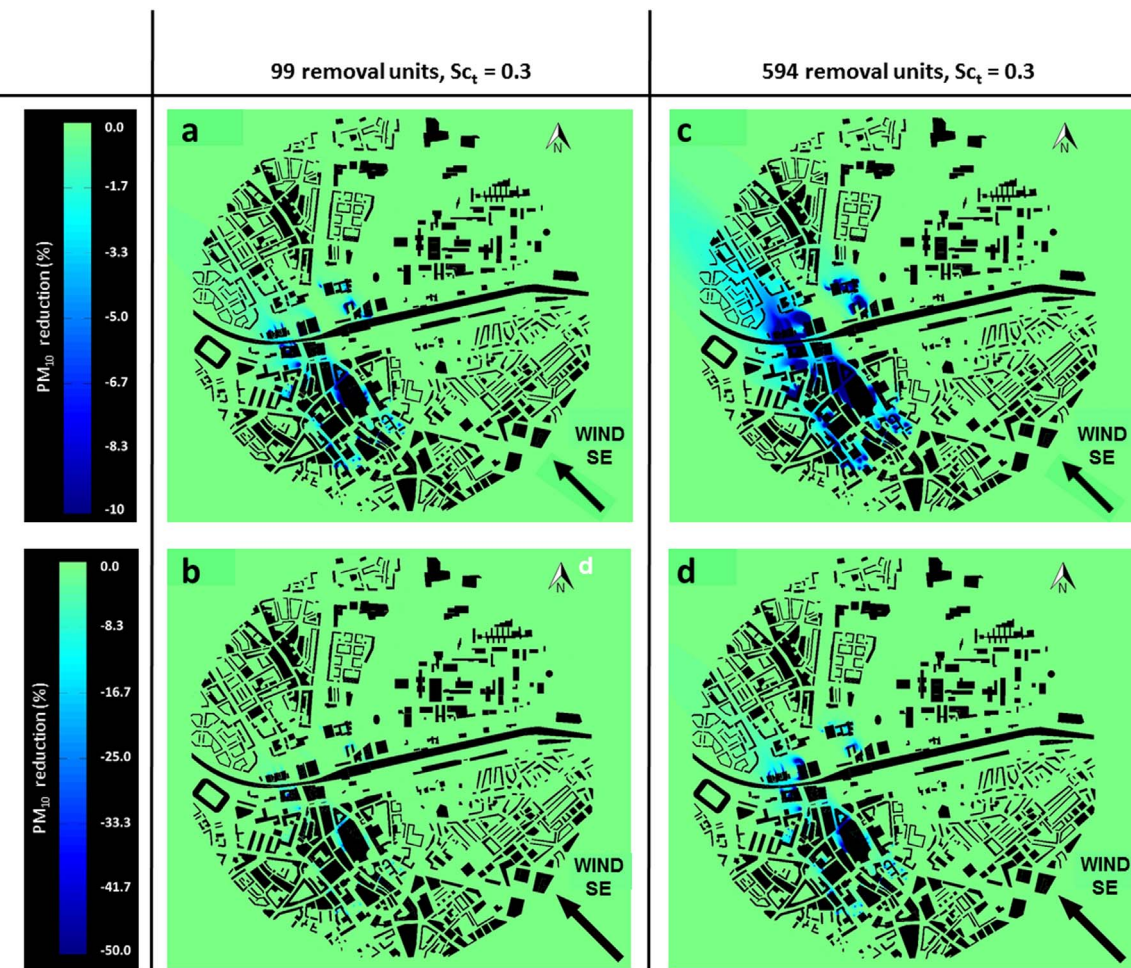


Fig. 19. Outdoor PM₁₀ reduction by removal units in the semi-enclosed parking garages: contours of in horizontal plane at 1.75 m height for Sc_t=0.3. (a,b) With 99 units installed. (c,d) With 594 units installed.

ing of traffic intensities and related emissions over the streets in the subareas and the equal temporal distribution of traffic intensities and related emissions over a 10 h period. The case study is not intended to reproduce a particular pollution episode. Although this approach and the related assumptions are common in CFD PM dispersion studies (see e.g. Jeanjean et al. (2016)), future work will focus on including more accurate dispersion boundary conditions, both for the streets and the parking garages, and on unsteady simulations, either with unsteady RANS or LES. This will allow simulating particular pollution episodes, which was out of the scope of the present study. In addition, thermal effects can be included, including short-wave and long-wave radiation, convection and local anthropogenic releases (e.g. Toparlar et al., 2015; Gromke et al., 2015).

The dispersion modeling in this paper adopted the simplified approach which excludes the specific treatment of aerosol dynamics and treats the particles as a gas. Although this approach has been widely adopted in CFD PM dispersion modeling (e.g. Kumar et al., 2009; Fuka and Brechler, 2012; Guo and Maghirang, 2012; Tong et al., 2016a, 2016b; Jeanjean et al., 2016), future much more advanced modeling work can consider including chemical formation (nucleation) and aerosol dynamics (coagulation, condensation, etc.).

PM deposition was not considered in this study. In reality, PM settling out will occur to a certain extent, which can be taken into account with the concept of deposition velocity. You et al. (2012) developed an empirical equation for indoor particle deposition velocities, and a similar approach could be followed for outdoor deposition. However, it should be noted that deposited PM could to some extent be re-entrained into the wind flow, e.g. by vehicle-induced turbulence.

The simulations were performed with two different Sc_t values, 0.3 and 0.7. It is well known that this parameter is a function of the flow field and the location in this flow field, and related to the relevant eddies dispersing the pollutant. As such, it is likely that the actual value will be different inside the removal units, inside the semi-enclosed garages and in the streets, and depend on street width and possibly also distance from the source. It should also be noted that in steady RANS modeling of dispersion, the value of Sc_t used is often based on fitting steady RANS results to experiments, in which the Sc_t is implicitly at least partly used to compensate for the deficiencies of steady RANS modeling, as outlined in the introduction of this paper.

In spite of these limitations, the present study has provided an assessment of the potential to reduce the traffic-induced fraction of outdoor PM concentration in urban areas by local removal inside semi-enclosed parking garages. A complex case study for a large urban area was performed, in which the semi-enclosed parking garages as well as the removal units were explicitly included in the computational domain and grid. The case study was supported by a detailed validation study based on an extensive set of gas dispersion wind-tunnel measurements for different building arrays with different wind directions and different Sc_t values. The case study was also performed for two different values of Sc_t to provide an indication about the related physical modeling uncertainty.

6. Summary and conclusions

Particulate matter (PM) is strongly associated with human morbidity and mortality. Traffic is one of the main sources of PM inside urban

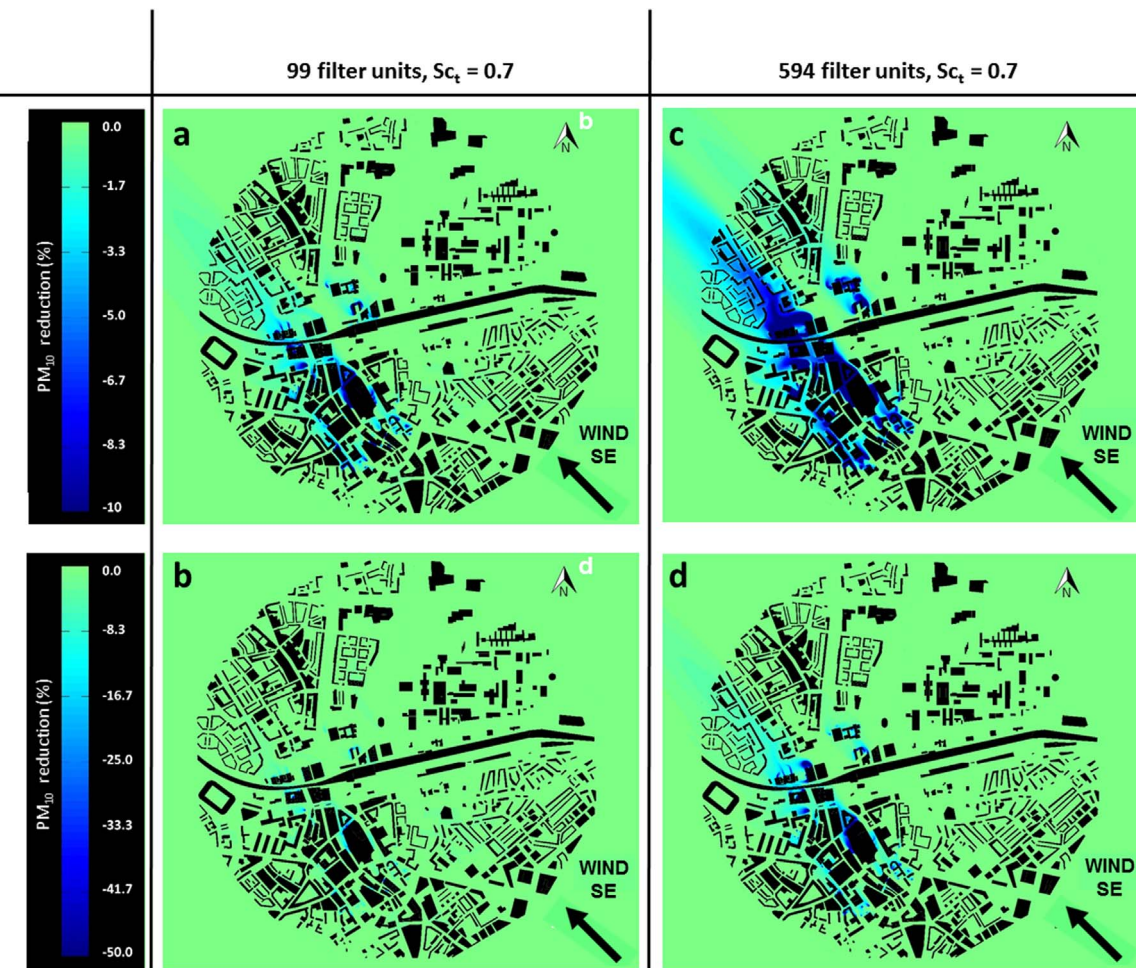


Fig. 20. Outdoor PM₁₀ reduction by removal units in the semi-enclosed parking garages: contours of in horizontal plane at 1.75 m height for $Sc_t=0.7$. (a,b) With 99 units installed. (c,d) With 594 units installed.

areas. Especially inside semi-enclosed parking garages, high PM concentrations can occur. This paper provided a preliminary assessment of the potential to reduce the traffic-induced fraction of outdoor PM concentrations in urban areas by local removal by electrostatic precipitation/positive ionization inside semi-enclosed parking garages. The assessment was performed by numerical simulations with computational fluid dynamics (CFD).

First, an extensive CFD validation study was conducted based on wind-tunnel experiments of wind-induced gas dispersion in three types of buildings arrays, for different wind directions and for two values of the turbulent Schmidt number ($Sc_t=0.3$ and 0.7). The simulations were performed with the 3D steady Reynolds-averaged Navier-Stokes (RANS) equations with the realizable k- ϵ model for closure and with an Eulerian advection-diffusion equation and the standard gradient-diffusion hypothesis for dispersion. Quite some previous studies have shown that steady RANS, in spite of its many limitations, can provide fairly accurate predictions of near-ground mean concentration fields by ground-level sources (generally less than factor 2 deviation) in densely built urban areas such as regular arrays of block-type buildings. This overall good performance of steady RANS was confirmed by the validation study in the present paper. The comparison of street concentrations by CFD simulations and wind-tunnel measurements indicated that none of the two Sc_t values performed best for all cases investigated, a finding that is in line with previous studies. This is not surprising as the appropriate value of the Sc_t number actually depends on the type of flow pattern and on the location in this flow pattern. However, apart from the case with $S_x=50$ mm, $S_y=100$ mm, the measured concentrations were generally situated between the simu-

lated concentrations by $Sc_t=0.3$ and $Sc_t=0.7$. Therefore, the validation study was used to support the CFD simulations for the case study of Eindhoven city center but these case study simulations were performed for both $Sc_t=0.3$ and $Sc_t=0.7$, in order to provide an indication of the physical modeling uncertainty involved.

Next, a CFD case study was performed for Eindhoven city center. The simulations were performed on a high-resolution high-quality grid that included the detailed geometry of 16 below-ground and above-ground semi-enclosed parking garages. Three cases were considered: a case without removal units, a case with a total of 99 units and a case with a total of 594 units inserted in the semi-enclosed parking garages. An efficiency of 0.7 of actual existing electrostatic precipitation/positive ionization units for PM₁₀ removal was employed. The 3D steady RANS equations were solved with the realizable k- ϵ model for closure for a reference wind speed $U_{10}=1$ m/s and for southeast wind direction. PM₁₀ dispersion was modeled in a simplified way, with an Eulerian advection-diffusion equation and the standard gradient-diffusion hypothesis. The specific treatment of aerosol dynamics was excluded from the computation, similar to several previous urban CFD PM dispersion studies. Traffic intensities on the streets and in the parking garages were converted to PM₁₀ source terms. The parking garages were ventilated with outdoor air according to Dutch building regulations. Every case was solved with both $Sc_t=0.3$ and 0.7. The case study was not intended to reproduce a particular pollution episode but to provide a preliminary indication of the potential reduction in outdoor PM₁₀ in the vicinity of the parking garages under a given set of representative meteorological and traffic conditions. With the specific choices and assumptions implemented in this case study, the results showed that

for the case with 594 filter units, local outdoor PM₁₀ reductions go up to 50% in the direct vicinity of the parking garages while reductions up to 10% are achieved for a substantial area further downstream. As a result, it can be concluded that local removal in semi-enclosed parking garages can be an effective strategy towards improved outdoor air quality. Future work will focus on more detailed modeling with a higher spatial and temporal resolution of traffic intensity and the related emissions.

Acknowledgements

The authors acknowledge the financial support from the Province of North Brabant in the Netherlands by the Smart Energy Regions initiative and the collaboration with Lia van de Vorle and dr.ir. Roel Gijsbers from the company ENS Technology in the framework of the project “Lungs of the City”. Twan van Hooff is currently a postdoctoral fellow of the Research Foundation – Flanders (FWO) and acknowledges its financial support (project FWO 12R9715N). The authors thank the anonymous reviewers for the very valuable review comments.

References

- Ahmad, K., Khare, M., Chaudhry, K.K., 2005. Wind tunnel simulation studies on dispersion at urban street canyons and intersections – a review. *J. Wind Eng. Ind. Aerodyn.* 93 (9), 697–717.
- Al, Z.T., Mak, C.M., 2015. Large-eddy Simulation of flow and dispersion around an isolated building: analysis of influencing factors. *Comput. Fluids* 118, 89–100.
- ANSYS Inc. 2011. ANSYS Fluent User Guide. Canonsburg.
- ASME, 2011. <http://journaltool.asme.org/Templates/JFENumberAccuracy.pdf>. Retrieved on 30 July 2011
- Baker, C.J., 2007. Wind engineering – Past, present and future. *J. Wind Eng. Ind. Aerodyn.* 95 (9–11), 843–870.
- Bazdidi-Tehrani, F., Ghafoori, A., Jadidi, M., 2013. Grid resolution assessment in large eddy simulation of dispersion around an isolated cubic building. *J. Wind Eng. Ind. Aerodyn.* 121, 1–15.
- Beelen, R., Raaschou-Nielsen, O., Stafoggia, M., et al., 2014. Effects of long-term exposure to air pollution on natural-cause mortality: an analysis of 22 European cohorts within the multicentre ESCAPE project. *Lancet* 383 (9919), 785–795.
- Block, M.L., Calderon-Garcidueñas, L., 2009. Air pollution: mechanisms of neuroinflammation and CNS disease. *Trends Neurosci.* 32 (9), 506–516.
- Blocken, B., Roels, S., Carmeliet, J., 2004. Modification of pedestrian wind comfort in the Silvertop Tower passages by an automatic control system. *J. Wind Eng. Ind. Aerodyn.* 92 (10), 849–873.
- Blocken, B., Carmeliet, J., Stathopoulos, T., 2007a. CFD evaluation of wind speed conditions in passages between parallel buildings—effect of wall-function roughness modifications for the atmospheric boundary layer flow. *J. Wind Eng. Ind. Aerodyn.* 95 (9–11), 941–962.
- Blocken, B., Stathopoulos, T., Carmeliet, J., 2007b. CFD simulation of the atmospheric boundary layer: wall function problems. *Atmos. Environ.* 41 (2), 238–252.
- Blocken, B., Stathopoulos, T., Saathoff, P., Wang, X., 2008a. Numerical evaluation of pollutant dispersion in the built environment: comparisons between models and experiments. *J. Wind Eng. Ind. Aerodyn.* 96 (10–11), 1817–1831.
- Blocken, B., Moonen, P., Stathopoulos, T., Carmeliet, J., 2008b. A numerical study on the existence of the Venturi-effect in passages between perpendicularly buildings. *J. Eng. Mech.* 134, 1021–1028.
- Blocken, B., Persoon, J., 2009. Pedestrian wind comfort around a large football stadium in an urban environment: CFD simulation, validation and application of the new Dutch wind nuisance standard. *J. Wind Eng. Ind. Aerodyn.* 97 (5–6), 255–270.
- Blocken, B., Stathopoulos, T., Carmeliet, J., Hensen, J.L.M., 2011. Application of CFD in building performance simulation for the outdoor environment: an overview. *J. Build. Perform. Simul.* 4 (2), 157–184.
- Blocken, B., Janssen, W.D., van Hooff, T., 2012. CFD simulation for pedestrian wind comfort and wind safety in urban areas: general decision framework and case study for the Eindhoven University campus. *Environ. Model. Softw.* 30, 15–34.
- Blocken, B., Tominaga, Y., Stathopoulos, T., 2013. CFD simulation of micro-scale pollutant dispersion in the built environment. *Build. Environ.* 64, 225–230.
- Blocken, B., 2014. 50 years of Computational Wind Engineering: past, present and future. *J. Wind Eng. Ind. Aerodyn.* 129, 69–102.
- Blocken, B., 2015. Computational Fluid Dynamics for urban physics: importance, scales, possibilities, limitations and ten tips and tricks towards accurate and reliable simulations. *Build. Environ.* 91, 219–245.
- Brauer, M., Lencar, C., Tamburic, L., Koehoorn, M., Demers, P., Karr, C., 2008. A cohort study of traffic-related air pollution impacts on birth outcomes. *Environ. Health Perspect.* 116 (5), 680–686.
- Brunekreef, B., Holgate, S.T., 2002. Air pollution and health. *Lancet* 360 (9341), 1233–1242.
- Buccolieri, R., Salizzoni, P., Soulhac, L., Garbero, V., Di Sabatino, S., 2015. The breathability of compact cities. *Urban Clim.* 13, 73–93.
- Casey, M., Wintergerste, T., 2000. Best Practice Guidelines, ERCOFTAC Special Interest Group on Quality and Trust in Industrial CFD, ERCOFTAC, Brussels.
- Cebeci, T., Bradshaw, P., 1977. *Momentum Transfer in Boundary Layers*. Hemisphere Publishing Corporation, New York.
- Chavez, M., Hajra, B., Stathopoulos, T., Bahloul, A., 2011. Near-field pollutant dispersion in the built environment by CFD and wind tunnel simulations. *J. Wind Eng. Ind. Aerodyn.* 99 (4), 330–339.
- Chavez, M., Hajra, B., Stathopoulos, T., Bahloul, A., 2012. Assessment of near-field pollutant dispersion: effect of upstream buildings. *J. Wind Eng. Ind. Aerodyn.* 104–106, 509–515.
- Chen, C., Zhao, B., 2011. Review of relationship between indoor and outdoor particles: i/o ratio, infiltration factor and penetration factor. *Atmos. Environ.* 45 (2), 275–288.
- Dejoan, A., Santiago, J.L., Martilli, A., Martin, F., Pinelli, A., 2010. Comparison between large-eddy simulation and Reynolds-averaged Navier–Stokes computations for the MUST field experiment. Part II: effects of incident wind angle deviation on the mean flow and plume dispersion. *Bound.-Layer Meteorol.* 135, 133–150.
- Di Sabatino, S., Buccolieri, R., Salizzoni, P., 2013. Recent advancements in numerical modelling of flow and dispersion in urban areas: a short review. *Int. J. Environ. Pollut.* 52 (3–4), 172–191.
- EEA, 2015. World premature deaths due to urban pollution from particulate matter and ground-level ozone. European Environment Agency. (<http://www.eea.europa.eu/data-and-maps/figures/world-premature-deaths-due-to>). Retrieved on 21/07/2016.
- Efthimiou, G.C., Berbekar, E., Harms, F., Bartzis, J.G., Leitl, B., 2015. Prediction of high concentrations and concentration distribution of a continuous point source release in a semi-idealized urban canopy using CFD-RANS modelling. *Atmos. Environ.* 100, 48–56.
- Eindhoven Municipality, 2015. (<http://www.eindhoven.nl/home.htm>). Retrieved on 21/07/2016.
- ENS, 2016a. Environmental Nano Solutions, (www.enstechnology.nl); Retrieved on 21/07/2016.
- ENS, 2016b. Personal communication. 21/07/2016.
- Flaherty, J.E., Stock, D., Lamb, B., 2007. Computational fluid dynamic simulations of plume dispersion in urban Oklahoma City. *J. Appl. Meteorol. Clim.* 46, 2110–2126.
- Franke, J., Hirsch, C., Jensen, A.G., Krius, H.W., Schatzmann, M., Westbury, P.S., Miles, S.D., Wisse, J.A., Wright, N.G., 2004. Recommendations on the use of CFD in wind engineering. In: van Beeck, J.P.A.J. (Ed.), *Proceedings of the International Conference on Urban Wind Engineering and Building Aerodynamics. COST Action C14, Impact of Wind and Storm on City Life Built Environment*. Von Karman Institute, Sint-Genesius-Rode, Belgium, 5–7 May 2004.
- Franke, J., Hellsten, A., Schlünzen, H., Carissimo, B., 2007. Best Practice Guideline for the CFD Simulation of Flows in the Urban Environment. COST Office Brussels, ISBN: 3-00-018312-4.
- Franke, J., Hellsten, A., Schlünzen, H., Carissimo, B., 2011. The COST 732 best practice guideline for CFD simulation of flows in the urban environment – A summary. *Int. J. Environ. Pollut.* 44 (1–4), 419–427.
- Fuka, V., Brechler, J., 2012. Large eddy simulation modelling of the dispersion of radioactive particulate matter. *Int. J. Environ. Pollut.* 48, 156–163.
- Garbero, V., Salizzoni, P., Soulhac, L., 2010. Experimental study of pollutant dispersion within a network of streets. *Bound.-Layer Meteorol.* 136, 457–487.
- Gousseau, P., Blocken, B., van Heijst, G.J.F., 2011a. CFD simulation of pollutant dispersion around isolated buildings: on the role of convective and turbulent mass fluxes in the prediction accuracy. *J. Hazard. Mater.* 194, 422–434.
- Gousseau, P., Blocken, B., Stathopoulos, T., van Heijst, G.J.F., 2011b. CFD simulation of near-field pollutant dispersion on a high-resolution grid: a case study by LES and RANS for a building group in downtown Montreal. *Atmos. Environ.* 45 (2), 428–438.
- Gousseau, P., Blocken, B., van Heijst, G.J.F., 2012. Large-Eddy Simulation of pollutant dispersion around a cubical building: analysis of the turbulent mass transport mechanism by unsteady concentration and velocity statistics. *Environ. Pollut.* 167, 47–57.
- Gousseau, P., Blocken, B., Stathopoulos, T., van Heijst, G.J.F., 2015. Near-field pollutant dispersion in an actual urban area: analysis of the mass transport mechanism by high-resolution Large Eddy Simulations. *Comput. Fluids* 114, 151–162.
- Gromke, C., Blocken, B., Janssen, W.D., Merema, B., van Hooff, T., Timmermans, H.J.P., 2015. CFD analysis of transpirational cooling by vegetation: Case study for specific meteorological conditions during a heat wave in Arnhem, Netherlands. *Build. Environ.* 83, 11–26.
- Guo, L., Maghirang, R.G., 2012. Numerical simulation of airflow and particle collection by vegetative barriers. *Eng. Appl. Comput. Fluid Mech.* 6 (1), 110–122.
- Hoek, G., Brunekreef, B., Goldbohm, S., Fischer, P., van den Brandt, P.A., 2002. Association between mortality of traffic-related air pollution in the Netherlands: a cohort study. *Lancet* 360 (9341), 1203–1209.
- Holmes, N.S., Morawska, L., 2006. A review of dispersion modelling and its application to the dispersion of particles: an overview of different dispersion models available. *Atmos. Environ.* 40 (30), 5902–5928.
- Janssen, W.D., Blocken, B., van Hooff, T., 2013. Pedestrian wind comfort around buildings: comparison of wind comfort criteria based on whole-flow field data for a complex case study. *Build. Environ.* 59, 547–562.
- Jeanjean, A.P.R., Monks, P.S., Leigh, R.J., 2016. Modelling the effectiveness of urban trees and grass on PM_{2.5} reduction via dispersion and deposition at a city scale. *Atmos. Environ.* 147, 1–10.
- Kim, S.R., Dominici, F., Buckley, T.J., 2007. Concentrations of vehicle-related air pollutants in an urban parking garage. *Environ. Res.* 105 (3), 291–299.
- Kumar, P., Garmory, A., Ketzel, M., Berkowicz, R., Britter, R., 2009. Comparative study of measured and modelled number concentrations of nanoparticles in an urban street canyon. *Atmos. Environ.* 43, 949–958.
- Kunzli, N., Kaiser, R., Medina, S., et al., 2000. Public-health impact of outdoor and traffic-related air pollution: a European assessment. *Lancet* 356 (9232), 795–801.

- Lateb, M., Meroney, R.N., Yataghene, M., Fellouah, H., Saleh, F., Boufadel, M.C., 2016. On the use of numerical modelling for near-field pollutant dispersion in urban environments – A review. *Environ. Pollut.* 208A, 271–283.
- Lauder, B.E., Spalding, D.B., 1974. The numerical computation of turbulent flows. *Comput. Methods Appl. Mech. Eng.* 3, 269–289.
- Leitl, B.M., Kastner-Klein, P., Rau, M., Meroney, R.N., 1997. Concentration and flow distributions in the vicinity of U-shaped buildings: wind-tunnel and computational data. *J. Wind Eng. Ind. Aerodyn.* 67 & 68, 745–755.
- Li, Y., Stathopoulos, T., 1997. Numerical evaluation of wind-induced dispersion of pollutants around a building. *J. Wind Eng. Ind. Aerodyn.* 67–68, 757–766.
- Li, Y., Stathopoulos, T., 1998. Computational evaluation of pollutant dispersion around buildings: estimation of numerical errors. *J. Wind Eng. Ind. Aerodyn.* 77 & 78, 619–630.
- Li, X.X., Liu, C.H., Leung, D.Y.C., Lam, K.M., 2006. Recent progress in CFD modelling of wind field and pollutant transport in street canyons. *Atmos. Environ.* 40 (29), 5640–5658.
- Liu, J., Niu, J., 2016. CFD simulation of the wind environment around an isolated high-rise building: An evaluation of SRANS, LES and DES models. *Build. Environ.* 96, 91–106.
- Majestic, B.J., Anbar, A.D., Herckes, P., 2009. Elemental and iron isotopic composition of aerosols collected in a parking structure. *Sci. Total Environ.* 407, 5104–5109.
- Meroney, R.N., Derickson, R., 2014. Virtual reality in wind engineering: the windy world within the computer. *J. Wind Eng. Ind. Aerodyn.* 11 (2), 11–26.
- Meroney, R.N., 2004. Wind tunnel and numerical simulation of pollution dispersion: a hybrid approach. Paper for Invited Lecture at the Croucher Advanced Study Institute, Hong Kong University of Science and Technology.
- Meroney, R.N., 2016. Ten questions concerning hybrid computational/physical model simulation of wind flow in the built environment. *Build. Environ.* 96, 12–21.
- Milliez, M., Carissimo, B., 2007. Numerical simulations of pollutant dispersion in an idealized urban area, for different meteorological conditions. *Bound.-Layer Meteorol.* 122 (2), 321–342.
- Murakami, S., 1990. Numerical simulation of turbulent flowfield around cubic model: current status and applications of k-e model and LES. *J. Wind Eng. Ind. Aerodyn.* 33 (1–2), 139–152.
- Murakami, S., 1993. Comparison of various turbulence models applied to a bluff body. *J. Wind Eng. Ind. Aerodyn.* 46 & 47, 21–36.
- Murakami, S., 1997. Current status and future trends in computational wind engineering. *J. Wind Eng. Ind. Aerodyn.* 67 & 68, 3–34.
- Murakami, S., Mochida, A., 1989. Three-dimensional numerical simulation of turbulent flow around buildings using the k-e turbulence model. *Build. Environ.* 24 (1), 51–64.
- Murakami, S., Mochida, A., Hayashi, Y., 1990. Examining the k-e model by means of a wind tunnel test and large-eddy simulation of the turbulence structure around a cube. *J. Wind Eng. Ind. Aerodyn.* 35, 87–100.
- Murakami, S., Mochida, A., Hayashi, Y., Sakamoto, S., 1992. Numerical study on velocity-pressure field and wind forces for bluff bodies by k-e, ASM and LES. *J. Wind Eng. Ind. Aerodyn.* 44 (1–3), 2841–2852.
- NEN, 2001. Dutch building regulations (Bouwbesluit), NEN 1087: Ventilation of buildings.
- Nordling, E., Berglund, N., Melen, E., Emenius, G., Hallberg, J., Nyberg, F., Pershagen, G., Svartengren, M., Wickman, M., Bellander, T., 2008. Traffic-related air pollution and childhood respiratory symptoms, function and allergies. *Epidemiology* 19 (3), 401–408.
- OECD, 2012. OECD Environmental Outlook to 2050: the Consequences of Inaction. 350 p. 9789264122246 (PDF); 9789264122161 (print).
- Obaidullah, M., Dyakov, I.V., Peeters, L., Bram, S., de Ruyck, J., 2013. Comparison of particle emissions from enclosed parking garages and streets. *Glob. Nest J.* 15 (4), 457–465.
- Paterson, D.A., Apelt, C.J., 1986. Computation of wind flows over three-dimensional buildings. *J. Wind Eng. Ind. Aerodyn.* 24, 192–213.
- Paterson, D.A., Apelt, C.J., 1990. Simulation of flow past a cube in a turbulent boundary layer. *J. Wind Eng. Ind. Aerodyn.* 35, 149–176.
- Pedersen, M., Giorgis-Allemand, L., Bernard, C., et al., 2013. Ambient air pollution and low birthweight: a European cohort study (ESCAPE). *Lancet Respir. Med.* 1 (9), 695–704.
- Pope, C.A., Dockery, D.W., 2006. Health effects of fine particulate air pollution: lines that connect. *J. Air Waste Manag. Assoc.* 56 (6), 709–742.
- Pospisil, J., Jicha, M., 2011. Particle re-suspension in street canyon with two-way traffic. *Int. J. Environ. Pollut.* 44 (1–4), 271–279.
- Raaschou-Nielsen, O., Andersen, Z.J., Beelen, R., et al., 2013. Air pollution and lung cancer incidence in 17 European cohorts: prospective analyses from the European Study of cohorts for Air Pollution Effects (ESCAPE). *Lancet Oncol.* 14 (9), 813–822.
- Ranft, U., Schikowski, T., Sugiri, D., Krutmann, J., Kramer, U., 2009. Long-term exposure to traffic-related particulate matter impairs cognitive function in the elderly. *Environ. Res.* 109 (8), 1004–1011.
- Richards, P.J., Hoxey, R.P., 1993. Appropriate boundary conditions for computational wind engineering models using the k-e turbulence model. *J. Wind Eng. Ind. Aerodyn.* 46 & 47, 145–153.
- Rijkswaterstaat, 2016. Emissiefactoren voor niet-snelwegen. (<https://www.rijksoverheid.nl/onderwerpen/luchtkwaliteit>). Retrieved on 21/7/2016.
- Robins, A., 2003. Wind tunnel dispersion modelling some recent and not so recent achievements. *J. Wind Eng. Ind. Aerodyn.* 91 (12–15), 1777–1790.
- Rodi, W., 1997. Comparison of LES and RANS calculations of the flow around bluff bodies. *J. Wind Eng. Ind. Aerodyn.* 69–71, 55–75.
- Rogge, W.F., Hildemann, L.M., Mazurek, M.A., Cass, G.R., Simoneit, B.R.T., 1993. Sources of fine organic aerosol. 3. Road dust, tire debris, and organometallic brake lining dust – roads as sources and sinks. *Environ. Sci. Technol.* 27 (9), 1892–1904.
- Samal, C.G., Gupta, D., Pathania, R., Mohan, S., Sureh, R., 2013. Air pollution in micro-environments: a case study of India Habitat Centre enclosed vehicular parking, New Delhi. *Indoor Built Environ.* 22 (4), 710–718.
- Samet, J.M., Dominici, F., Curriero, F.C., Coursac, I., Zeger, S.L., 2000. Fine particulate air pollution and mortality in 20 US cities, 1987–1994. *N. Engl. J. Med.* 343 (24), 1742–1749.
- Shao, J., Liu, J., Zhao, J., 2012. Evaluation of various non-linear k-e models for predicting wind flow around an isolated high-rise building within the surface boundary layer. *Build. Environ.* 57, 145–155.
- Shih, T.H., Liou, W.W., Shabbir, A., Yang, Z., Zhu, J., 1995. A new k-e eddy viscosity model for high Reynolds number turbulent flows. *Comput. Fluids* 24, 227–238.
- Solari, G., 2007. The International Association for Wind Engineering (IAWE): progress and prospects. *J. Wind Eng. Ind. Aerodyn.* 95, 813–842.
- Stathopoulos, T., 1997. Computational wind engineering: past achievements and future challenges. *J. Wind Eng. Ind. Aerodyn.* 67–68, 509–532.
- Tominaga, Y., Murakami, S., Mochida, A., 1997. CFD prediction of gaseous diffusion around a cubic model using a dynamic mixed SGS model based on composite grid technique. *J. Wind Eng. Ind. Aerodyn.* 67–68, 827–841.
- Tominaga, Y., Stathopoulos, T., 2007. Turbulent Schmidt numbers for CFD analysis with various types of flowfield. *Atmos. Environ.* 41 (37), 8091–8099.
- Tominaga, Y., Mochida, A., Murakami, S., Sawaki, S., 2008a. Comparison of various revised k-e models and LES applied to flow around a high-rise building model with 1:1:2 shape placed within the surface boundary layer. *J. Wind Eng. Ind. Aerodyn.* 96 (4), 389–411.
- Tominaga, Y., Mochida, A., Yoshie, R., Kataoka, H., Nozu, T., Yoshikawa, M., Shirasawa, T., 2008b. AIJ guidelines for practical applications of CFD to pedestrian wind environment around buildings. *J. Wind Eng. Ind. Aerodyn.* 96 (10–11), 1749–1761.
- Tominaga, Y., Stathopoulos, T., 2009. Numerical simulation of dispersion around an isolated cubic building: comparison of various types of k-e models. *Atmos. Environ.* 43 (20), 3200–3210.
- Tominaga, Y., Stathopoulos, T., 2010. Numerical simulation of dispersion around an isolated cubic building: Model evaluation of RANS and LES. *Build. Environ.* 45 (10), 2231–2239.
- Tominaga, Y., Stathopoulos, T., 2012. CFD modeling of pollution dispersion in building array: evaluation of turbulent scalar flux modeling in RANS model using LES results. *J. Wind Eng. Ind. Aerodyn.* 104–106, 484–491.
- Tominaga, Y., Stathopoulos, T., 2013. CFD simulation of near-field pollutant dispersion in the urban environment: a review of current modelling techniques. *Atmos. Environ.* 79, 716–730.
- Tominaga, Y., 2015. Flow around a high-rise building using steady and unsteady RANS CFD: effect of large-scale fluctuations on the velocity statistics. *J. Wind Eng. Ind. Aerodyn.* 142, 93–103.
- Tominaga, Y., Stathopoulos, T., 2016. Ten questions concerning modeling of near-field pollutant dispersion in the built environment. *Build. Environ.* 105, 390–402.
- Tong, Z., Baldauf, R.W., Isakov, V., Deshmukh, P., Zhang, K.M., 2016b. Roadside vegetation barrier designs to mitigate near-road air pollution impacts. *Sci. Total Environ.* 541, 920–927.
- Tong, Z., Chen, Y., Malkawi, A., Adamkiewicz, G., Spengler, J.D., 2016a. Quantifying the impact of traffic-related air pollution on the indoor quality of a naturally ventilated building. *Environ. Int.* 89–90, 138–146.
- Topalar, Y., Blocken, B., Vos, P., van Heijst, G.J.F., Janssen, W.D., van Hooff, T., Montazeri, H., Timmermans, H.J.P., 2015. CFD simulation and validation of urban microclimate: a case study for Bergpolder Zuid, Rotterdam. *Build. Environ.* 83, 79–90.
- Tucker, P.G., Mosquera, A., 2001. NAFEMS introduction to grid and mesh generation for CFD. NAFEMS CFD Working Group, R0079, pp. 56.
- You, R.Y., Zhao, B., Chen, C., 2012. Developing an empirical equation for modeling particle deposition velocity onto inclined surfaces in indoor environments. *Aerosol Sci. Technol.* 46 (10), 1090–1099.
- Valavanidis, A., Fiotakis, K., Vlachogianni, T., 2008. Airborne particulate matter and human health: toxicological assessment and importance of the size and composition of particles for oxidative damage and carcinogenic mechanisms. *J. Environ. Sci. Health Part C – Environ. Carcinog. Ecotoxicol. Rev.* 26 (4), 339–362.
- van Hooff, T., Blocken, B., 2010. Coupled urban wind flow and indoor natural ventilation modelling on a high-resolution grid: a case study for the Amsterdam Arena stadium. *Environ. Model. Softw.* 25 (1), 51–65.
- Vukovic, G., Urosevic, M.A., Razumencic, I., Kuzmanoski, M., Pergal, M., Skrivanj, S., Popovic, A., 2014. Air quality in urban parking garages (PM₁₀, major and trace elements, PAHs): instrumental measurements vs. active moss biomonitoring. *Atmos. Environ.* 85, 31–40.
- WHO, 2005. Air quality guidelines, global update 2005. Particulate matter, ozone, nitrogen dioxide and sulfur dioxide. ISBN 92 890 2192 6.
- WHO, 2014. Ambient(outdoor) air quality and health. Fact sheet N°313, updated March 2014. (<http://www.who.int/mediacentre/factsheets/fs313/en/>).
- WHO, 2016. (http://www.who.int/gho/phe/outdoor_air_pollution/exposure_text/en/). Retrieved on 21/08/2016.
- Wieringa, J., 1992. Updating the Davenport roughness classification. *J. Wind Eng. Ind. Aerodyn.* 41–44, 357–368.
- Yoshie, R., Mochida, A., Tominaga, Y., Kataoka, H., Harimoto, K., Nozu, T., Shirasawa, T., 2007. Cooperative project for CFD prediction of pedestrian wind environment in the Architectural Institute of Japan. *J. Wind Eng. Ind. Aerodyn.* 95 (9–11), 1551–1578.
- Zhang, G.S., Li, T.T., Luo, M., Liu, J.F., Liu, Z.R., Bai, Y.H., 2008. Air pollution in the microenvironment of parked new cars. *Build. Environ.* 43 (3), 315–319.